

1
2
3
4
5
6
7
8
9
10
11
12
13
14
15
16
17
18
19
20
21
22
23
24
25
26

Bacteria establish an aqueous living space as a crucial virulence mechanism

Xiu-Fang Xin¹, Kinya Nomura¹, Kyaw Aung^{1,2}, André C. Velásquez¹, Jian Yao^{1,*}, Freddy Boutrot³, Jeff H. Chang⁴, Cyril Zipfel³, Sheng Yang He^{1,2,5,6 †}

Affiliations:

¹Department of Energy Plant Research Laboratory, Michigan State University, East Lansing, MI 48824, USA

²Howard Hughes Medical Institute, Gordon and Betty Moore Foundation, Michigan State University, East Lansing, MI 48824, USA

³The Sainsbury Laboratory, Norwich Research Park, NR4 7UH Norwich, UK

⁴Department of Botany and Plant Pathology and Center for Genome Research and Biocomputing, Oregon State University, Corvallis, OR 97331, USA

⁵Department of Plant Biology, Michigan State University, East Lansing, MI 48824, USA

⁶Plant Resilience Institute, Michigan State University, East Lansing, MI 48824, USA

* Current address: Department of Biological Sciences, Western Michigan, Kalamazoo, MI 49008, USA

†Correspondence to: Sheng Yang He; email: hes@msu.edu

27 **Abstract**

28

29 **High humidity has a profound influence on the development of numerous**
30 **phyllosphere diseases in crop fields and natural ecosystems, but the**
31 **molecular basis of this humidity effect is not understood. Previous studies**
32 **emphasize immune suppression as a key step in bacterial pathogenesis. Here**
33 **we show that humidity-dependent, pathogen-driven establishment of an**
34 **aqueous intercellular space (apoplast) is another crucial step in bacterial**
35 **infection of the phyllosphere. Bacterial effectors, such as *Pseudomonas***
36 ***syringae* HopM1, induce establishment of the aqueous apoplast and are**
37 **sufficient to transform non-pathogenic *P. syringae* strains into virulent**
38 **pathogens in immune-deficient *Arabidopsis* under high humidity. *Arabidopsis***
39 **quadruple mutants simultaneously defective in a host target (MIN7) of**
40 **HopM1 and in pattern-triggered immunity could not only recapitulate the**
41 **basic features of bacterial infection, but also exhibit humidity-dependent**
42 **dyshomeostasis of the endophytic commensal bacterial community in the**
43 **phyllosphere. These results highlight a new conceptual framework for**
44 **understanding diverse phyllosphere-bacterial interactions.**

45

46 **Introduction**

47 The terrestrial phyllosphere (the above-ground parts of plants) represents one of the
48 most important habitats on Earth for microbial colonization. Although the vast majority
49 of phyllosphere microbes exhibit benign commensal associations and maintain only
50 modest populations, adapted phyllosphere pathogens can multiply aggressively under
51 favorable environmental conditions and cause devastating diseases. In crop fields,
52 phyllosphere bacterial disease outbreaks typically occur after rainfalls and a period of
53 high humidity¹⁻³, consistent with the famous “disease triangle” (host-pathogen-
54 environment) dogma formulated more than 50 years ago⁴. The molecular basis of the

55 profound effect of high humidity on bacterial infection of the phyllosphere is not
56 understood.

57

58 Many plant and animal pathogenic bacteria, including the model phyllosphere bacterial
59 pathogen *Pseudomonas syringae*, carry a type III secretion system (T3SS), which is
60 used to deliver disease-promoting “effector” proteins into the host cell as a primary
61 mechanism of pathogenesis^{5,6}. Studies of how individual type III effectors promote
62 bacterial disease in plants and animals show that effector-mediated suppression of host
63 immunity is a common theme in both plant-bacterial⁷⁻⁹ and animal-bacterial
64 interactions^{10,11}. However, due to the apparent molecular complexities in bacterial
65 diseases, the fundamental question as to what minimal set of host processes that must
66 be subverted to allow basic bacterial pathogenesis to occur has not been answered in
67 any plant or animal pathosystem.

68

69 **Immune-suppression and pathogenesis**

70 To test the hypothesis that host immunity may be the only process that needs to be
71 subverted for bacterial pathogenesis in the phyllosphere, we performed infection assays
72 in *Arabidopsis* polymutants severely defective in multiple immune pathways: (i)
73 *fls2/efr/cerk1 (fec)*, which is mutated in three major pattern recognition receptor (PRR)
74 genes relevant to *P. syringae* pv. *tomato (Pst)* DC3000 infection¹², (ii) *bak1-5/bkk1-*
75 *1/cerk1 (bbc; see Methods)*, which is compromised in immune signaling downstream of
76 multiple PRRs^{13,14}, and (iii) *dde2/ein2/pad4/sid2 (deps)*, which is defective in all three
77 major defense hormone pathways (salicylic acid, jasmonate and ethylene)¹⁵. Two
78 nonpathogenic mutant derivatives of *Pst* DC3000 were used: the *hrcC* mutant
79 (defective in type III secretion)¹⁶ and the DC3000D28E mutant, in which the T3SS
80 remains intact, but 28 of 36 type III effectors are deleted¹⁷. As shown in Fig. 1a, *hrcC*
81 and DC3000D28E mutants grew very poorly not only in wild-type Col-0, but also in
82 immune-compromised mutants when infiltrated into the apoplast, suggesting that host
83 immunity is unlikely to be the only process subverted by *Pst* DC3000 during infection.

84

85 **High humidity required for pathogenesis**

86 During the active pathogenesis phase, phyllosphere bacterial pathogens such as *Pst*
87 DC3000 live mainly in the air-filled apoplast, which is connected directly to open air
88 through epidermal pores called stomata. The water status inside the apoplast could
89 therefore be influenced by air humidity during pathogen infection. In crop fields,
90 phyllosphere bacterial disease outbreaks typically occur after rainfalls and a period of
91 high humidity^{1-3,18}, following the “disease triangle” dogma in plant pathology. In
92 addition, one of the earliest and common symptoms of phyllosphere bacterial diseases
93 is the appearance of “water soaking” in infected tissues, although whether water-
94 soaking plays an active role in bacterial pathogenesis remains unclear. These key
95 phenomena could be demonstrated in the laboratory. Whereas *Pst* DC3000 multiplied to
96 a very high level under high humidity (~95%; mimicking high humidity after rains in
97 crop fields), it multiplied to a much lower level under low humidity (< 60%) (Fig. 1b),
98 as reflected also in a lower disease severity (Fig. 1c). The ability of *Pst* DC3000 to
99 multiply increased as humidity rose; in contrast, the *hrcC* mutant multiplied poorly
100 under all tested humidity conditions (Fig. 1d). The most aggressive infection by *Pst*
101 DC3000 was associated with the appearance, usually within one day after infection, of
102 water soaking in the infected *Arabidopsis* leaves under high humidity (Fig. 1e). Water-
103 soaked spots could also be observed in *Pst* DC3000-infected leaves of another host
104 species, tomato (Fig. 1f). Real-time imaging (Supplementary Video 1) showed that the
105 initial water-soaked spots mark the areas of later disease symptoms (necrosis and
106 chlorosis), and revealed, interestingly, that water soaking was a transient process and it
107 disappeared before the onset of late disease symptoms. Using a *Pst* DC3000 strain
108 tagged with a luciferase reporter (DC3000-*lux*¹⁹), we found that water soaking areas
109 and luciferase signals are detected nonuniformly across the leaf, but they overlap
110 extensively (Fig. 1g, Extended Data Fig. 1), revealing that water-soaked areas are
111 where bacteria multiply aggressively in the phyllosphere before the onset of late disease
112 symptoms.

113

114 ***P. syringae* water-soaking effectors**

115 The DC3000D28E mutant never caused water soaking under any condition (e.g., high
116 humidity/inoculum). We therefore transformed each of the 28 *Pst* DC3000 effector
117 genes, individually, back to the DC3000D28E mutant to identify the effector(s) that
118 cause water soaking. Most effectors did not (see Fig. 2a for *avrPto*, as an example); but
119 *hopM1* and *avrE* (together with their respective type III secretion chaperone genes
120 *shcM* and *avrF*) did (Fig. 2a). We found this result interesting because, although HopM1
121 and AvrE show no sequence similarity, they were previously shown to be functionally
122 redundant in virulence and they are highly conserved in diverse *P. syringae* strains
123 and/or other phytopathogenic bacteria^{20,21}. Moreover, transgenic overexpression of
124 6xHis:HopM1²² or 6xHis:AvrE²³ under control of dexamesathone (DEX)-inducible
125 promoter (10 μM DEX used) also caused water soaking under high humidity (Fig. 2b).
126 In contrast, transgenic expression of AvrPto, like D28E (*avrPto*), did not. These results
127 show that HopM1 and AvrE, either delivered by bacteria or when overexpressed
128 transgenically inside the plant cells, are each sufficient to cause water soaking.

129
130 Bacterial mutant analysis showed that HopM1 and AvrE are necessary for *Pst* DC3000 to
131 cause water soaking during infection, as the *avrE/hopM1* double mutant²⁰ could not
132 cause water soaking, even when the inoculum of the *avrE/hopM1* mutant was adjusted
133 to reach a similar population with *Pst* DC3000 when water soaking was assessed (Fig.
134 2c). In contrast, *Pst* DC3000 and the *avrE* and *hopM1* single mutants²⁰ caused strong
135 initial water soaking (Extended Data Fig. 2a) and later disease symptoms (Extended
136 Data Fig. 2b) and multiplied aggressively in a high humidity-dependent manner, while
137 the *avrE/hopM1* double mutant multiplied poorly regardless of the humidity setting
138 (Fig. 2d). Transgenic expression of 6xHis:HopM1 in Arabidopsis (in these experiments
139 0.1 nM was used to induce low-level expression of HopM1 so that HopM1 alone does
140 not cause extensive water soaking) restored the ability of the *avrE/hopM1* double
141 mutant to cause water soaking and multiply highly under high humidity (Extended Data
142 Fig. 2c, d). These results revealed that, unlike the other 34 effectors present in the

143 *avrE/hopM1* double mutant, the virulence functions of HopM1 and AvrE are uniquely
144 dependent on external high humidity.

145
146 Why would the virulence functions of HopM1 and AvrE be dependent on the external
147 humidity? We hypothesized that perhaps the primary function of HopM1 and AvrE is to
148 create an aqueous apoplast *per se* (i.e., bacteria “prefer” to living in an aqueous
149 environment in the apoplast), the maintenance of which requires high humidity as the
150 leaf apoplast is directly connected to open air through stomata. If so, it may be possible
151 to substitute the function of HopM1 and AvrE by simply providing water to the apoplast.
152 To directly test this hypothesis, we performed transient water supplementation
153 experiments in which Col-0 plants infiltrated with the *avrE/hopM1* mutant were kept
154 water-soaked, transiently, for the first 12 h to 16 h to mimic the kinetics of transient
155 water soaking normally occurring during *Pst* DC3000 infection (Supplementary Video 1).
156 Remarkably, transient apoplast water supplementation was sufficient to restore the
157 multiplication (100- to 1000-fold) of the *avrE/hopM1* mutant almost to the level of *Pst*
158 DC3000 (Fig. 2e), as well as appearance of severe disease symptoms (Fig. 2f). As
159 controls, *Pst* DC3000, the *hrcC* mutant and CUCPB5452 (which contains *avrE* and
160 *hopM1* genes but has much reduced virulence due to deletion of other type III
161 effectors²⁴) grew only slightly better (<10 fold) with transient water-supplementation
162 (Fig. 2e). These results demonstrate that the primary virulence function of HopM1 and
163 AvrE can be effectively substituted by supplying water, transiently, to the apoplast.

164

165 **HopM1’s host target in water soaking**

166 To investigate the mechanism by which HopM1 creates aqueous apoplast, we focused
167 on the host targets of HopM1 in Arabidopsis. We have previously shown that HopM1 is
168 targeted to the trans-Golgi-network/early endosome (TGN/EE) in the host cell and
169 mediates proteasome-dependent degradation of several host proteins, including MIN7
170 (also known as BEN1), which is a TGN/EE-localized ADP ribosylation factor-guanine
171 nucleotide exchange factor involved in vesicle trafficking^{22,25,26}. Although the *min7*
172 mutant plant partially allows increased bacterial multiplication^{22,25}, the exact role of

173 MIN7 during pathogen infection remains enigmatic. A previous study showed that
174 HopM1's virulence function is fundamentally different from that of canonical immune-
175 suppressing effectors, such as AvrPto¹⁷. In light of our discovery of HopM1's primary
176 role in creating water-soaking in this study, we tested the intriguing possibility that
177 MIN7 may be a key player in modulating apoplast water soaking in response to
178 bacterial infection. Excitingly, we found that the *min7* mutant plant allowed apoplast
179 water soaking to occur in the absence of HopM1/AvrE (i.e., during infection by the *avrE*
180 */hopM1* mutant; Fig. 3a, Extended Data Fig. 3c), and allowed the *avrE*/*hopM1* mutant
181 to multiply (Extended Data Fig. 3a, b). Thus, genetic removal of MIN7 is sufficient to
182 mimic the virulence function of HopM1, albeit partially, in causing apoplast water
183 soaking. The *min7* mutant plant is defective in endocytic recycling of plasma membrane
184 (PM) proteins and has an abnormal PM²⁶, suggesting that HopM1 degrades MIN7
185 possibly to compromise host PM integrity as a mechanism to create an infection-
186 promoting aqueous apoplast (Extended Data Fig. 4).

187
188 If apoplast water soaking is an essential step of pathogenesis, we hypothesized that
189 plants may have evolved defense mechanisms to counter it. Indeed, we found that *Pst*
190 DC3000 (*avrRpt2*)-triggered effector-triggered immunity (ETI)²⁷ completely blocked
191 water-soaking, even when the inoculum of *Pst* DC3000 (*avrRpt2*) was raised to reach a
192 population similar to *Pst* DC3000 when water soaking was assessed (Fig. 3b, c,
193 Extended Data Fig. 5a-b). When transferred from high (~95%) to low (~50%)
194 humidity, *Pst* DC3000 (*avrRpt2*)-infected leaves quickly wilted, indicating extensive ETI-
195 associated programmed cell death. In contrast, *Pst* DC3000-infected, water-soaked
196 leaves returned to pre-infection healthy appearance (Fig. 3b), indicating little host cell
197 death during apoplast water soaking. Furthermore, *Pst* DC3000 (*avrRpt2*)-triggered ETI
198 stabilized the MIN7 protein (Fig. 3d). These results therefore uncovered a previously
199 unrecognized battle between bacterial virulence (creating apoplast water soaking) and
200 host defense (preventing apoplast water soaking), in part linked to MIN7 stability, to
201 take control of apoplast water availability.

202

203 **Reconstitution of *P. syringae* infection**

204 The discovery of apoplast water soaking as a key process of bacterial pathogenesis
205 prompted us to investigate a new model in which PTI suppression and creation of
206 apoplast water soaking are two principal pathogenic processes sufficient for bacterial
207 infection of the phyllosphere. To test this hypothesis, we infected Col-0 and two PTI-
208 compromised mutant plants (i.e., *fec* and *bbc*) with DC3000D28E, DC3000D28E
209 (*avrPto*) or DC3000D28E (*hopM1/shcM*) and found that only DC3000D28E
210 (*hopM1/shcM*), but not DC3000D28E or DC3000D28E (*avrPto*), caused strong water
211 soaking, multiplied aggressively (almost to the *Pst* DC3000 level) and produced
212 prominent disease symptoms in the *fec* and *bbc* mutant plants (Fig. 4a-c) in a high
213 humidity-dependent manner (Fig. 4d). Furthermore, unlike PTI mutants, the *npr1-6*
214 mutant plant, which is defective in salicylic acid-dependent defense (Extended Data Fig.
215 6a-c), could not rescue the ability of DC3000D28E (*hopM1/shcM*) to multiply (Fig. 4a).
216 Thus, a combination of defective PTI and presence of an aqueous-apoplast-inducing
217 effector (HopM1) could almost fully convert a non-pathogenic mutant into a virulent
218 pathogen in the Arabidopsis phyllosphere.

219

220 If immune suppression and creation of apoplast water soaking are two principal
221 pathogenic processes sufficient for bacterial infection of the phyllosphere, we reasoned
222 that we might be able to construct a multi-host-target mutant that simulates the two
223 processes. Such mutant plant might allow an otherwise nonpathogenic mutant
224 bacterium (e.g., the *hrcC* mutant) to colonize the phyllosphere, thereby reconstituting
225 basic features of a phyllosphere bacterial infection. For this purpose, we mutated the
226 *MIN7* gene in PTI mutants (*fec* and *bbc*) and generated *min7/fls2/efr/cerk1 (mfec)* and
227 *min7/bak1-5/bkk1-1/cerk1 (mbbc)* quadruple mutants using CRISPR technology (see
228 Methods; Extended Data Fig. 7a). The quadruple mutant plants display a similar
229 morphology as wild type Col-0 plants (Extended Data Fig. 7b) and have a tendency of
230 showing some water-soaking spots, especially in mature leaves, under high humidity
231 (Extended Data Fig. 7c, d). Excitingly, these mutants allow the nonpathogenic *hrcC*
232 mutant to multiply aggressively under high (~95%) humidity, to a final population that

233 was ~100 fold higher than in Col-0 plants 5 days after inoculation, with the *mbbc* plants
234 showing a greater susceptibility than the *mfec* plants (Fig. 5a). In addition, in these
235 quadruple mutant plants, the *hrcC* mutant induced prominent disease chlorosis and
236 necrosis (Fig. 5b, Extended Data Fig. 7e), which were not observed for the *hrcC* strain
237 in Col-0, *min7* or PTI mutants. Thus, a dual disruption of MIN7 and PTI signaling is
238 sufficient to reconstitute the basic features of a model phyllosphere bacterial disease.
239 Consistent with this conclusion, transient water supplementation to the leaf apoplast
240 was sufficient to enhance the growth of the *hrcC* mutant in the *bbc* triple mutant, but
241 not in Col-0 plants (Fig. 5c). To our knowledge, this is the first infectious model disease,
242 in plant or animal, for which basic pathogenesis has been reconstituted using
243 biologically relevant host target mutants.

244

245 **Dyshomeostasis of commensal bacteria**

246 The inability of the nonpathogenic *hrcC* mutant to multiply aggressively in wild-type
247 phyllosphere resembles that of the commensal bacterial community that resides in the
248 apoplast of healthy leaves. Consistent with this, only low levels of the endophytic
249 phyllosphere bacterial community were detectable in wild type Col-0 plants (Fig. 5d).
250 However, after plants were shifted from regular growth conditions (~60% relative
251 humidity, day 0; Fig. 5d) to high humidity conditions (~95% relative humidity), the
252 *mfec* and *mbbc* quadruple mutant plants, but not Col-0 plants, allowed excessive
253 proliferation of the endogenous endophytic bacterial community (Fig. 5d, Extended
254 Data Table 1), in a high humidity dependent manner (Extended Data Fig. 8a).
255 Furthermore, the excessive proliferation of the endophytic bacterial community was
256 associated with mild tissue chlorosis and necrosis in some leaves (Extended Data Fig.
257 8b). We found this result intriguing as a recent study showed that overgrowth of a
258 beneficial root-colonizing fungus in immune-compromised (against fungal pathogens)
259 plants also led to harmful effects in *Arabidopsis*²⁸, illustrating a potentially common
260 theme that the levels of commensal and beneficial microbiota must be strictly controlled
261 by the host for optimal plant health. Future comprehensive *in planta* 16S rRNA
262 amplicon-based analysis will be needed to determine whether there are also humidity-

263 dependent changes in the composition of commensal bacterial communities in the Col-
264 0, *mfec* and *mbbc* plants.

265

266 **Discussion**

267 Results from this study suggest a new conceptual framework for understanding
268 phyllosphere-bacterial interactions (Fig. 5e). Specifically, we have identified PTI
269 signaling and MIN7, presumably via vesicle trafficking, as two key components of the
270 elusive host barrier that functions to limit excessive and potentially harmful proliferation
271 of nonpathogenic microbes (e.g., *hrcC* mutant) in the phyllosphere. Pathogenic
272 bacteria, like *Pst* DC3000, have evolved T3SS effectors not only to disarm PTI signaling,
273 but also to establish an aqueous living space in a humidity-dependent manner in order
274 to aggressively colonize the phyllosphere. This new conceptual framework integrates
275 host, pathogen and environmental factors, providing a critical insight into the enigmatic
276 basis of the profound effect of humidity on the development of numerous bacterial
277 diseases, consistent with the “disease triangle” dogma in plant pathology.

278

279 Prior to this study, humidity was commonly thought to promote bacterial movements on
280 the plant surface and invasion into plant tissues. Our study, however, revealed a
281 striking and previously unrecognized effect of high humidity on the function of bacterial
282 effectors inside the plant apoplast. An aqueous apoplast could potentially facilitate the
283 flow of nutrients to bacteria, promote the spread/ egression of bacteria, and/or affect
284 apoplastic host defense responses, the latter of which may explain some of the
285 previously observed effects of HopM1, AvrE and MIN7 on plant immunity^{21,23,25} and
286 suggest a potential “cross-talk” between plant immune responses and water availability.

287

288 Most of our current knowledge on plant-pathogens and plant-microbiome interactions
289 are derived from studies under limited laboratory conditions. This study illustrates a
290 need for future research to consider the dynamic climate conditions in which plants and
291 microbes live in nature in order to uncover new biological phenomena involved in host-
292 microbe interactions. Research that unravels the molecular bases of environmental

293 influences of disease development should help us understand the severity, emergence
294 and/or disappearance of infectious diseases in crop fields and natural ecosystems,
295 especially in light of the dramatically changing drought/humidity patterns associated
296 with global climate change.

297

298 **Methods**

299

300 **Plant materials and bacterial strains**

301 *Arabidopsis thaliana* plants were grown in the “Arabidopsis Mix” soil (equal parts of
302 SUREMIX [Michigan Grower Products Inc., Galesburg, MI], medium vermiculate and
303 perlite; autoclaved once) or Redi-Earth soil (Sun Gro[®] Horticulture) in environmentally-
304 controlled growth chambers, with relative humidity at 60%, temperature at 22 °C and
305 12h light/12h dark cycle. Five-week-old plants were used for bacterial inoculation and
306 disease assays.

307

308 The *bak1-5/bkk1-1/cerk1* mutant plant was generated by crossing the *bak1-5/bkk1-1*
309 mutant¹⁴ with the *cerk1* mutant²⁹. PCR-based genotyping was performed in F₂ progeny
310 to obtain a homozygous triple mutant. The *npr1-6* (Fig. 4a) mutant was the
311 SAIL_708_F09 line ordered from the Arabidopsis Biological Resource Center, and
312 confirmed to be a knock-out mutant and defective in SA signaling (Extended Data Fig.
313 6).

314

315 **Bacterial disease assays**

316 Syringe-infiltration and dip-inoculation were performed. Briefly, *Pst* DC3000 and mutant
317 strains were cultured in Luria-Marine (LM³⁰) medium containing 100mg/L rifampicin
318 (and/or other antibiotics if necessary) at 28°C to OD₆₀₀ of 0.8 - 1.0. Bacteria were
319 collected by centrifugation and re-suspended in sterile water. Cell density was adjusted
320 to OD₆₀₀ = 0.2 (~1x10⁸ cfu/ml). For syringe-infiltration, bacterial suspension was
321 further diluted to cell densities of 1x10⁵ to 1x10⁶ cfu/ml. Unless stated otherwise,

322 infiltrated plants were first kept under ambient humidity for 1-2 h for water to
323 evaporate, and, after the plant leaves returned to pre-infiltration appearance, plants
324 were kept under high humidity (~95%; by covering plants with domes) or other
325 specified humidity settings for disease to develop. For dip-inoculation, plants were
326 dipped in the bacterial suspension of $OD_{600} = 0.2$, with 0.025% Silwet L-77 added, and
327 then kept under high humidity (~95%) immediately for disease to develop.

328

329 Different humidity settings were achieved by placing a plastic dome over a flat (in which
330 plants are grown) with different degrees of opening. A humidity/temperature Data
331 Logger (Lascar) was placed inside the flat to record the humidity and/or temperature
332 over the period of disease assay.

333

334 For quantification of *Pst* DC3000 bacterial populations, Arabidopsis leaves were surface-
335 sterilized in 75% ethanol and rinsed in sterile water twice. Leaf disks were taken using
336 a cork borer (9.5mm in diameter) and ground in sterile water. Colony-forming units
337 were determined by serial dilutions and plating on LM plates containing 100mg/L
338 rifampicin. Two leaf disks from two leaves were pooled together as one technical
339 replicate, and 4 technical replicates are included in each biological experiment.
340 Experiments were repeated at least three times.

341

342 **CRISPR-Cas9-mediated mutation of the *MIN7* gene**

343 The one-plasmid CRISPR-Cas9 cloning system³¹ was used to mutate *MIN7* in the
344 *fls2/efr/cerk1* and *bak1-5/bkk1-1/cerk1* plants. *MIN7*-sgRNA primers containing target
345 mutation regions were as follows, with *MIN7* sequence underlined.

346 *MIN7*-sgRNA-F: GATTGATCATTTGGAAGGGGATCC

347 *MIN7*-sgRNA-R: AAACGGATCCCTTCCAAATGATC

348 The constructs containing *MIN7*-sgRNA and Cas9 were cloned in pCAMBIA1300, which
349 were then mobilized into *Agrobacterium tumefaciens* for plant transformation. For
350 genotyping of *MIN7*-mutated lines, total DNA was extracted from individual lines and

351 the regions containing the CRISPR target sites were amplified by PCR using the
352 following primers:

353 *MIN7*-sgRNA-F2: GATGCTGCTTTGGATTGTCTTC

354 *MIN7*-sgRNA-R2: AATGGCTCCCATGCACTGCGATA

355 For genotyping, the PCR products were digested by the *Bam*HI restriction enzyme and
356 plant lines showing an (partially or completely) uncut band were chosen. The PCR
357 products of putative homozygous T₂ lines, identified based on a lack of cutting by
358 *Bam*HI, were sequenced. The lines showing a frame-shift mutation and an absence of
359 *Cas9* gene based on PCR using the following primers were identified as homozygous
360 lines. The T₃ and T₄ progeny of homozygous lines were used for disease assays.

361 Primers for PCR-amplifying *Cas9* gene:

362 *Cas9*-F: CCAGCAAGAAATTCAAGGTGC

363 *Cas9*-R: GCACCAGCTGGATGAACAGCTT

364

365 **Imaging of bacterial colonization with luciferase assay**

366 Four-week-old Arabidopsis Col-0 plants were dip-inoculated with *Pst* DC3000 or *Pst*
367 DC3000-*lux* strain. The infected plants were fully covered with plastic dome to maintain
368 high humidity. Leaves were excised from the infected plants 2 days post inoculation and
369 the light signals were captured by a charge-coupled device (CCD) using ChemiDoc™ MP
370 system (Bio-Rad).

371

372 **MIN7 protein blot**

373 Arabidopsis leaves were syringe-infiltrated with bacteria or H₂O and kept under high
374 humidity (~95%) for 24h. Leaf disks were homogenized in 2xSDS buffer, boiled for 5
375 min and centrifuged at 10,000 x *g* for 1 min. Supernatants containing the total protein
376 extracts were subjected to separation by SDS-polyacrylamide gel electrophoresis

377 (PAGE). A MIN7 antibody²² was used in the western blot to detect the MIN7 protein.
378 Uncropped blot/gel images are included in Supplementary Figure 1.

379

380 **Bacterial community quantification**

381 Five-week old plants were sprayed with H₂O and covered with a plastic dome to keep
382 high humidity (~95%) for 5 days. To quantify the endophytic bacterial community,
383 leaves were detached, sterilized in 75% ethanol for 1 min (Extended Data Fig. 9) and
384 rinsed in sterile water twice. Leaves were weighed and ground in sterile water using a
385 TissueLyser (Qiagen; at the frequency of 30 times per second for 1 min) in the
386 presence of 3 mm Zirconium oxide grinding beads (Glen Mills; 5 beads in each tube).
387 After serial dilutions, bacterial suspensions were plated on R2A plates, which were kept
388 at 22°C for 4 days before colonies were counted. Colony-forming units were normalized
389 to tissue fresh weight.

390

391 **16S rRNA amplicon sequence analysis of endophytic bacterial community**

392 The Col-0, *mfec* and *mbbc* plants were sprayed with water and kept under high
393 humidity (~95%) for 5 days. Leaves were surface-sterilized in 75% ethanol for 1 min
394 and rinsed in sterile water twice. Leaves from four plants were randomly selected (2
395 leaves from each plants; 8 leaves in total) and were divided in 4 tubes (2 leaves in each
396 tube) and ground in sterile water. Bacterial suspensions were diluted (Col-0 samples
397 were diluted to 10⁻³ and *mfec* and *mbbc* samples were diluted to 10⁻⁵) and, for each
398 genotype, 15 µl suspension from each tube of the right dilution (10⁻³ dilution for Col-0
399 and 10⁻⁵ for *mfec* and *mbbc*) were pooled together and plated on R2A plates, which
400 were kept at 22°C for 4 days. Fifty colonies from each genotype were randomly picked
401 and genomic DNA was extracted and PCR was performed with AccuPrime high-fidelity
402 Taq DNA polymerase (Invitrogen) and primers 799F/1392R³³ to amplify bacterial 16S
403 rRNA gene. The PCR product was sequenced and taxonomy of each bacterium (family
404 level) was determined by Ribosomal Database Project at Michigan State University
405 (<https://rdp.cme.msu.edu/>)³⁴.

406

407 **Data analysis, statistics and experimental repeats**

408 The specific statistical method used, the sample size and the results of statistical
409 analyses are described in the relevant figure legends. Sample size was determined
410 based on experimental trials and in consideration of previous publications on similar
411 experiments to allow for confident statistical analyses. The Student's two-tailed *t*-test
412 was performed for comparison of means between two data points. One-way or two-way
413 ANOVA with Tukey's test was used for multiple comparisons within a dataset, with *p*
414 value set at 0.05. ANOVA analysis was performed with the GraphPad Prism software.

415

416 **Data Availability**

417 The bacterial 16S rRNA sequences in Extended Data Table 1 have been deposited in the
418 National Center for Biotechnology Information (NCBI) GenBank database under
419 accession numbers KX959313-KX959462. Other data that support the findings of this
420 study are available from the corresponding author upon request.

421

422 **References**

- 423 1 Miller, S., Rowe, R. & Riedel, R. Bacterial spot, speck, and canker of Tomatoes. *Ohio*
424 *State University Extension Fact Sheet HYG-3120-96* (1996)
- 425 2 Pernezny, K. & Zhang, S. Bacterial speck of tomato. *University of Florida IFAS Extension*
426 *PP-10* (2005).
- 427 3 Schwartz, H. F. Bacterial diseases of beans. *Colorado State University Extension. Fact*
428 *Sheet No: 2.913*. (2011)
- 429 4 Stevens, R. B. *Plant Pathology, an Advanced Treatise*. Vol. 3 (Academic Press, New
430 York, 1960)
- 431 5 Buttner, D. & He, S. Y. Type III protein secretion in plant pathogenic bacteria. *Plant*
432 *Physiol.* **150**, 1656-1664 (2009)
- 433 6 Galán, J. & Collmer, A. Type III secretion machines: bacterial devices for protein
434 delivery into host cells. *Science* **284**, 1322-1328 (1999)
- 435 7 Asai, S. & Shirasu, K. Plant cells under siege: plant immune system versus pathogen
436 effectors. *Curr. Opin. Plant Biol.* **28**, 1-8 (2015)
- 437 8 Dou, D. & Zhou, J. M. Phytopathogen effectors subverting host immunity: different foes,
438 similar battleground. *Cell Host Microbe* **12**, 484-495 (2012)
- 439 9 Macho, A. P. & Zipfel, C. Targeting of plant pattern recognition receptor-triggered
440 immunity by bacterial type-III secretion system effectors. *Curr. Opin. Microbiol.* **23**, 14-
441 22 (2015)
- 442 10 Asrat, S., Davis, K. M. & Isberg, R. R. Modulation of the host innate immune and
443 inflammatory response by translocated bacterial proteins. *Cell Microbiol.* **17**, 785-795
444 (2015)

- 445 11 Sperandio, B., Fischer, N. & Sansonetti, P. J. Mucosal physical and chemical innate
446 barriers: Lessons from microbial evasion strategies. *Sem. Immunol.* **27**, 111-118 (2015)
- 447 12 Gimenez-Ibanez, S., Ntoukakis, V. & Rathjen, J. P. The LysM receptor kinase CERK1
448 mediates bacterial perception in Arabidopsis. *Plant Signal. Behav.* **4**, 539-541 (2009)
- 449 13 Macho, A. P. & Zipfel, C. Plant PRRs and the activation of innate immune signaling. *Mol.*
450 *Cell* **54**, 263-272 (2014)
- 451 14 Schwessinger, B. *et al.* Phosphorylation-dependent differential regulation of plant
452 growth, cell death, and innate immunity by the regulatory receptor-like kinase BAK1.
453 *PLoS Genet.* **7**, e1002046 (2011)
- 454 15 Tsuda, K., Sato, M., Stoddard, T., Glazebrook, J. & Katagiri, F. Network properties of
455 robust immunity in plants. *PLoS Genet.* **5**, e1000772 (2009)
- 456 16 Yuan, J. & He, S. Y. The *Pseudomonas syringae* Hrp regulation and secretion system
457 controls the production and secretion of multiple extracellular proteins. *J. Bacteriol.* **178**,
458 6399-6402 (1996)
- 459 17 Cunnac, S. *et al.* Genetic disassembly and combinatorial reassembly identify a minimal
460 functional repertoire of type III effectors in *Pseudomonas syringae*. *Proc. Natl. Acad. Sci.*
461 *USA* **108**, 2975-2980 (2011)
- 462 18 Hirano, S. S. & Upper, C. D. Population biology and epidemiology of *Pseudomonas*
463 *syringae*. *Annu. Rev. Phytopathol.* **28**, 155-177 (1990)
- 464 19 Fan, J., Crooks, C. & Lamb, C. High-throughput quantitative luminescence assay of the
465 growth in planta of *Pseudomonas syringae* chromosomally tagged with *Photobacterium*
466 *luminescens* luxCDABE. *Plant J.* **53**, 393-399 (2008)
- 467 20 Badel, J. L., Shimizu, R., Oh, H. S. & Collmer, A. A *Pseudomonas syringae* pv. *tomato*
468 avrE1/hopM1 mutant is severely reduced in growth and lesion formation in tomato. *Mol.*
469 *Plant Microbe Interact.* **19**, 99-111 (2006)
- 470 21 DebRoy, S., Thilmony, R., Kwack, Y. B., Nomura, K. & He, S. Y. A family of conserved
471 bacterial effectors inhibits salicylic acid-mediated basal immunity and promotes disease
472 necrosis in plants. *Proc. Natl. Acad. Sci. USA* **101**, 9927-9932 (2004)
- 473 22 Nomura, K. *et al.* A bacterial virulence protein suppresses host innate immunity to cause
474 plant disease. *Science* **313**, 220-223 (2006)
- 475 23 Xin, X. F. *et al.* *Pseudomonas syringae* effector Avirulence protein E localizes to the host
476 plasma membrane and down-regulates the expression of the *NONRACE-SPECIFIC*
477 *DISEASE RESISTANCE1/HARPIN-INDUCED1-LIKE13* gene required for antibacterial
478 immunity in Arabidopsis. *Plant Physiol.* **169**, 793-802 (2015)
- 479 24 Wei, C. F. *et al.* A *Pseudomonas syringae* pv. *tomato* DC3000 mutant lacking the type III
480 effector HopQ1-1 is able to cause disease in the model plant *Nicotiana benthamiana*.
481 *Plant J.* **51**, 32-46 (2007)
- 482 25 Nomura, K. *et al.* Effector-triggered immunity blocks pathogen degradation of an
483 immunity-associated vesicle traffic regulator in Arabidopsis. *Proc. Natl. Acad. Sci. USA*
484 **108**, 10774-10779 (2011)
- 485 26 Tanaka, H., Kitakura, S., De Rycke, R., De Groot, R. & Friml, J. Fluorescence imaging-
486 based screen identifies ARF GEF component of early endosomal trafficking. *Curr. Biol.*
487 **19**, 391-397 (2009)
- 488 27 Kim, M. G. *et al.* Two *Pseudomonas syringae* type III effectors inhibit RIN4-regulated
489 basal defense in Arabidopsis. *Cell* **121**, 749-759 (2005)
- 490 28 Hiruma, K. *et al.* Root Endophyte *Colletotrichum tofieldiae* Confers Plant Fitness Benefits
491 that Are Phosphate Status Dependent. *Cell* **165**, 464-474 (2016)

- 492 29 Miya, A. *et al.* CERK1, a LysM receptor kinase, is essential for chitin elicitor signaling in
493 Arabidopsis. *Proc. Natl. Acad. Sci. USA* **104**, 19613-19618 (2007)
- 494 30 Preston, G., Deng, W. L., Huang, H. C. & Collmer, A. Negative regulation of hrp genes in
495 *Pseudomonas syringae* by HrpV. *J. Bacteriol.* **180**, 4532-4537 (1998)
- 496 31 Feng, Z. *et al.* Multigeneration analysis reveals the inheritance, specificity, and patterns
497 of CRISPR/Cas-induced gene modifications in Arabidopsis. *Proc. Natl. Acad. Sci. USA*
498 **111**, 4632-4637 (2014)
- 499 32 Hauck, P., Thilmony, R. & He, S. Y. A *Pseudomonas syringae* type III effector
500 suppresses cell wall-based extracellular defense in susceptible Arabidopsis plants. *Proc.*
501 *Natl. Acad. Sci. USA* **100**, 8577-8582 (2003)
- 502 33 Bai Y. *et al.* Functional overlap of the Arabidopsis leaf and root microbiota. *Nature* **528**,
503 364-369 (2015)
- 504 34 Wang, Q., Garrity, G. M., Tiedje, J. M. & Cole. J. R. Naïve Bayesian Classifier for
505 Rapid Assignment of rRNA Sequences into the New Bacterial Taxonomy. *Appl Environ*
506 *Microbiol.* **73**, 5261-5267 (2007)
- 507

508 **Supplementary Information** is linked to the online version of the paper at
509 www.nature.com/nature.

510

511 **Acknowledgements**

512 We thank He lab members for insightful discussions and constructive suggestions. We
513 thank James Kremer for help with setting up real-time disease imaging experiments and
514 advice on 16S rRNA amplicon sequencing, Koichi Sugimoto for providing tomato plants
515 (cv. Castle Mart), and Caitlin Thireault for technical help. This project was supported by
516 funding from Gordon and Betty Moore Foundation (GBMF3037), National Institutes of
517 Health (GM109928) and the Department of Energy (the Chemical Sciences,
518 Geosciences, and Biosciences Division, Office of Basic Energy Sciences, Office of
519 Science; DE-FG02-91ER20021 for infrastructural support). C.Z acknowledges support
520 from The Gatsby Charitable Foundation.

521

522 **Author Contributions**

523 X-F.X, K.N, and S.Y.H designed the experiments. K.A performed the *Pst* DC3000-*lux*
524 imaging experiment. A.C.V performed biological repeats of bacterial infection
525 experiments shown in Fig. 1a. J.Y characterized an unpublished plant mutant line. X-F.X
526 and K.N performed all other experiments, including bacterial infections, protein blotting

527 and generation of Arabidopsis *mfec* and *mbbc* mutant lines. F.B and C.Z contributed
528 unpublished plant mutant materials. J.H.C contributed unpublished *Pst* DC3000 effector
529 constructs. X-F.X and S.Y.H wrote the manuscript with input from all co-authors.

530

531 **Author Information**

532 Reprints and permissions information is available at www.nature.com/reprints. The
533 authors declare no competing financial interests. Readers are welcome to comment on
534 the online version of the paper. Correspondence and requests for materials should be
535 addressed to S.Y.H. (hes@msu.edu).

536 **Figure 1:** Full-scale *Pst* DC3000 infection requires high humidity and is tightly
537 associated with apoplast “water soaking”. See Methods for syringe-infiltration or dip-
538 inoculation of plants described in all figures. **a**, Bacterial populations in Col-0,
539 *fls2/efr/cerk1 (fec)*, *bak1-5/bkk1-1/cerk1 (bbc)* and *dde2/ein2/pad4/sid2 (deps)* leaves
540 2 days post infiltration with bacteria at 1×10^6 cfu/ml. Humidity: ~95%. Two-way ANOVA
541 with Tukey’s test (p value set at 0.05) was performed. No significant differences were
542 found for DC3000 populations in different plant genotypes (indicated by the same letter
543 a), whereas differences were found for *hrcC* or DC3000D28E populations in different
544 plant genotypes, as indicated by different letters of the same type (a’ vs. b’ for *hrcC*
545 and a” vs. b” for DC3000D28E). $n=4$ technical replicates; error bars, mean \pm s.d.
546 Experiments were repeated three times with similar results. **b-c**, Bacterial populations
547 **(b)** and disease symptoms **(c)** 3 days post infiltration with *Pst* DC3000 at 1×10^5 cfu/ml.
548 * indicates a significant difference determined by Student’s *t*-test (two-tailed); ***,
549 $p=1.08 \times 10^{-6}$. $n=4$ technical replicates; error bars, mean \pm s.d. Experiments were
550 repeated four times with similar results. **d**, Bacterial populations in Col-0 leaves 3 days
551 post infiltration with bacteria at 1×10^5 cfu/ml. Statistical analysis was the same as in **a**.
552 Significant differences were found for DC3000 populations under different humidities, as
553 indicated by different letters (a, b, c and d). No significant differences were found in
554 *hrcC* populations (indicated by the same letter a’). $n=3$ technical replicates; error bars,
555 mean \pm s.d. Experiments were repeated three times with similar results. **e**, Pictures of
556 the abaxial sides of Col-0 leaves 24 h post infiltration with *Pst* DC3000 at 1×10^6 cfu/ml.
557 Humidity: ~95%. Dark spots on the leaf indicate water soaking spots. Red boxes
558 indicate “zoomed-in” regions. **f**, Picture of a tomato leaf (cv. Castle Mart) 3 days after
559 infiltration with *Pst* DC3000 at 1×10^4 cfu/ml. Humidity: ~95%. Yellow circles in **e** and **f**
560 indicate infiltration sites. Images were representative of water-soaked leaves from more
561 than four plants. **g**, Col-0 plants were dip-inoculated with bacteria at 2×10^8 cfu/ml.
562 Humidity: ~95%. Bacterial colonies in inoculated leaves were visualized 2 days later by
563 a charge-coupled device (upper panel) and pictures of leaves were taken to show water
564 soaking spots (middle panel). Bottom panel shows merged images, with the artificial

565 red color labeling *Pst* DC3000-*lux* bacteria. Experiments were repeated three times.
566 Images were representative of leaves from more than four plants.

567

568 **Figure 2:** Type III effectors AvrE and HopM1 are necessary and sufficient to cause
569 water soaking. **a**, Pictures of Col-0 leaves 24 h post infiltration with bacteria ($1-2 \times 10^8$
570 cfu/ml). Humidity: $\sim 95\%$. **b**, Pictures of leaves of transgenic 6xHis:HopM1²²,
571 6xHis:AvrE²³ or AvrPto³² plants after spray with 10 μ M dexamethasone (DEX; to induce
572 effector gene expression). Humidity: $\sim 95\%$. Col-0 or Col-0 *g*/plants were non-
573 transgenic parental controls. Images were representative of leaves from more than four
574 plants. **c**, Pictures of Col-0 leaves (left) and bacterial populations (right) 24 h post
575 infiltration with *Pst* DC3000 (1×10^6 cfu/ml) or the *avrE*/*hopMT* strain (1×10^7 cfu/ml).
576 Humidity: $\sim 95\%$. Student's *t*-test (two-tailed) was performed; ns, not significant
577 ($p=0.104$). $n=3$ biological replicates; error bars, mean \pm s.d. Experiments were repeated
578 three times. **d**, Bacterial populations in Col-0 plants 3 days post infiltration with bacteria
579 at 2×10^5 cfu/ml. *** indicates a significant difference ($p=1.07 \times 10^{-6}$, 8.07×10^{-7} and
580 5.95×10^{-7} for DC3000, the *avrE* mutant and the *hopMT* mutant, respectively) of
581 bacterial population between different humidities, as determined by Student's *t*-test
582 (two-tailed); ns, not significant ($p=0.13$). $n=4$ technical replicates; error bars,
583 mean \pm s.d. Experiments were repeated three times. **e-f**, Bacterial populations (**e**) and
584 leaf pictures (**f**) in Col-0 leaves 3 days post infiltration with bacteria at 1×10^5 cfu/ml. In
585 the "- H₂O" treatment, plants were air-dried normally (for ~ 2 h) and then kept under
586 high humidity ($\sim 95\%$). In the "+H₂O" treatment, plants were kept under high (80-
587 95%) humidity after syringe-infiltration to allow slow evaporation of water (for ~ 16 h,
588 until no visible apoplast water can be seen). ** ($p=8.29 \times 10^{-3}$ and 1.14×10^{-3} for DC3000
589 and *hrcC*, respectively) and *** ($p=7.61 \times 10^{-7}$ and 9.82×10^{-4} for *avrE*/*hopMT* and
590 CUCPB5452, respectively) indicate significant differences between "- H₂O" and "+H₂O"
591 treatments as determined by Student's *t*-test (two-tailed). $n=3$ technical replicates;
592 error bars, mean \pm s.d. Experiments were repeated three times.

593

594 **Figure 3:** Effects of MIN7 and effector-triggered immunity on water soaking. **a**, The
595 *min7* leaves, but not Col-0 leaves, showed partial water soaking 48 h after dip-
596 inoculation with the *avrE/hopM1* mutant at 1×10^8 cfu/ml. Humidity: ~95%. Water
597 soaking disappeared after transition to low humidity (~25%) to allow evaporation of
598 apoplast water. Images were representative of leaves from more than four plants. **b-c**,
599 ETI blocks apoplast water soaking. Col-0 and *rps2* leaves were infiltrated with
600 *Pst* DC3000 (1×10^6 cfu/ml) or *Pst* DC3000 (*avrRpt2*) (1×10^7 cfu/ml for Col-0 and 1×10^6
601 cfu/ml for *rps2* plants). Plants were kept under high humidity (~95%) for 24 h to
602 observe water soaking and then shifted to low humidity (~50%) for 4 h to observe ETI-
603 associated tissue collapse. Pictures were taken before and after low humidity exposure
604 (**b**) and bacterial populations were determined 24 h post infiltration to show similar
605 population levels (**c**). Statistical analysis of data in **c** was performed by one-way ANOVA
606 with Tukey's test (p value set at 0.05), and no significant difference was detected. $n=3$
607 technical replicates; error bars, mean \pm s.d. Experiments were repeated three times. **d**,
608 MIN7 protein is stabilized during ETI revealed by immunoblot. Col-0 or *min7* leaves
609 were infiltrated with bacteria (1×10^7 cfu/ml²⁵) or H₂O and kept under high humidity
610 (~95%) for 24 h before protein extraction. Asterisk indicates a non-specific band.
611 Coomassie blue staining shows equal loading. See Supplementary Figure 1 for cropping.

612 **Figure 4:** *hopM1/shcM* transform the non-pathogenic DC3000D28E mutant into a
613 highly virulent pathogen in PTI-deficient mutant plants in a humidity-dependent
614 manner. **a-c**, Bacterial populations (**a**) and disease symptoms (**b**) 3 days post
615 infiltration with bacteria indicated at 1×10^6 cfu/ml. Humidity: ~95%. Statistical analysis
616 was performed by one-way ANOVA with Tukey's test (p value set at 0.05). Bacterial
617 populations indicated by different letters (i.e., a, b and c) are significantly different (ab
618 is not significantly different from a or b). $n=4$ technical replicates; error bars,
619 mean \pm s.d. Experiments were repeated three times. Water-soaking symptom was
620 recorded 24 h post inoculation (**c**). **d**, Bacterial populations 3 days post infiltration with
621 DC3000D28E (*hopM1/shcM*) at 1×10^6 cfu/ml under indicated humidities. Statistical
622 analysis was the same as in (**a**). Bacterial populations indicated by different letters (i.e.,

623 a, b and c) are significantly different. $n=4$ technical replicates; error bars, mean \pm s.d.
624 Experiments were repeated three times. Images were representative of leaves from at
625 least four plants.

626 **Figure 5:** Disease reconstitution experiments. **a-b**, The *hrcC* bacterial populations 5
627 days **(a)** and disease symptoms 10 days post dip-inoculation **(b)** in Col-0, *fec*, *bbc*,
628 *min7*, *min7/fls2/efr/cerk1* (*mfec*) and *min7/bak1-5/bkk1-1/cerk1* (*mbbc*) plants.
629 Humidity: $\sim 95\%$. Statistical analysis was performed by one-way ANOVA with Tukey's
630 test (p value set at 0.05). Bacterial populations indicated by different letters (i.e., a, b, c
631 and d) are significantly different (ad is not significantly different from a or d). $n=4$
632 technical replicates; error bars, mean \pm s.d. Experiments were repeated four times. **c**,
633 The *hrcC* bacterial populations in Col-0 and *bbc* leaves 3 days post infiltration with
634 bacteria at 1×10^6 cfu/ml. The "- H₂O" and "+ H₂O" conditions are the same as in Fig.
635 2e. Statistical analysis was performed by one-way ANOVA with Tukey's test (p value set
636 at 0.05). Bacterial populations indicated by different letters (i.e., a, b and c) are
637 significantly different (ab is not significantly different from a or b). $n=3$ technical
638 replicates; error bars, mean \pm s.d. Experiments were repeated three times. **d**, The Col-0,
639 *fec*, *bbc*, *min7*, *mfec* and *mbbc* plants were mock-sprayed with H₂O and kept under
640 high humidity ($\sim 95\%$). On day 0 (before water spray) and day 5, total populations of
641 the endophytic bacterial community were quantified by counting colony-forming units
642 on R2A plates, after surface sterilization of leaves with 75% ethanol, leaf
643 homogenization and serial dilutions. Statistical analysis is the same as in **(a)**. Bacterial
644 populations indicated by different letters (i.e., a and b) are significantly different. $n=4$
645 technical replicates; error bars, mean \pm s.d. Experiments were repeated three times. **e**, A
646 new model for *Pst* DC3000 pathogenesis in Arabidopsis. Dashed arrows indicate a
647 possible interplay, at spatial and temporal scales, between "immune suppression" and
648 "wet apoplast" during pathogenesis.

649 **Extended Data Table 1: Endophytic bacterial taxa in Col-0, *mfec* and *mbbc***
650 **plants.** *, not detected (nd). See the Methods section for 16S rRNA amplicon
651 sequencing procedures.

652

653 **Extended Data Figure 1:** Water soaking does not affect luminescence signal. Col-0
654 plants were dip-inoculated with bacteria at 2×10^8 cfu/ml, and kept under high humidity
655 (~95%) for 2 days. Imaging was performed in the same way as in Fig. 1g. Water-
656 soaked leaves were air-dried for about 2 h and imaged again (right panel). Images
657 were representative of leaves from more than four plants.

658 **Extended Data Figure 2: a-b,** The virulence of the *avrE/hopM1* mutant is
659 insensitive to humidity settings. **a,** Col-0 plants were syringe-infiltrated with indicated
660 bacteria at 2×10^5 cfu/ml. Inoculated plants were kept under high (~95%) humidity, and
661 pictures were taken 24 h post infiltration. **b,** Col-0 plants were syringe-infiltrated with
662 *Pst* DC3000, the *avrE* mutant, the *hopM1* mutant or the *avrE/hopM1* mutant at 2×10^5
663 cfu/ml. Inoculated plants were kept under high (~95%) or low (20-40%) humidity.
664 Pictures were taken 3 days post inoculation. Images were representative of leaves from
665 more than four plants. **c-d,** The 6xHis:HopM1 transgenic plants were infiltrated with 0.1
666 nM DEX, the *avrE/hopM1* mutant (at 1×10^5 cfu/ml) or both. H₂O was infiltrated as
667 control. Infiltrated plants were kept at high humidity (~95%). Leaf pictures were taken
668 24 h post infiltration (**c**) and bacterial populations were determined 3 days post
669 infiltration (**d**). * indicates a significant difference, as determined by Student's *t*-test;
670 (two-tailed); ***, $p=1.03 \times 10^{-5}$. $n=6$ technical replicates from three independent
671 experiments ($n=2$ in each experiment); error bars, mean \pm s.d.

672

673 **Extended Data Figure 3:** Bacterial multiplication and water soaking in Col-0 and the
674 *min7* mutant. **a,** The Col-0 and *min7* plants were dip-inoculated with *Pst* DC3000, the
675 *avrE/hopM1* mutant or the *hrcC* mutant at 1×10^8 cfu/ml. Bacterial populations were
676 determined 4 days post inoculation. * indicates a significant difference between Col-0
677 and *min7* plants, as determined by Student's *t*-test (two-tailed); *, $p=1.61 \times 10^{-2}$ and

678 3.12×10^{-2} for DC3000 and *hrcC*, respectively; ***, $p=1.41 \times 10^{-4}$ for *avrE/hopM1*. $n=4$
679 technical replicates; error bars, mean \pm s.d. Experiments were repeated three times. **b-**
680 **c**, The Col-0 and *min7* plants were syringe-infiltrated with *Pst* DC3000, the *avrE*
681 */hopM1* mutant or the *hrcC* mutant at 1×10^6 cfu/ml. Bacterial populations were
682 determined 3 days post inoculation (**b**) and leaf pictures were taken 38 h after
683 infiltration to show water soaking in *min7* leaves (**c**). * indicates a significant difference
684 between Col-0 and *min7* plants, as determined by Student's *t*-test (two-tailed); **,
685 $p=1.63 \times 10^{-3}$ for *avrE/hopM1*; ns, not significant ($p=0.72$ and 0.14 for DC3000 and
686 *hrcC*, respectively). $n=3$ technical replicates; error bars, mean \pm s.d. Experiments were
687 repeated three times. Images were representative of leaves from more than four
688 plants.

689

690 **Extended Data Figure 4:** *Pst* DC3000 delivers a total of 36 effectors into the plant
691 cell. Many effectors, including AvrPto, appear to suppress pattern-triggered immunity
692 (PTI). AvrPto inhibits pattern recognition receptor (PRR) function⁸. Two conserved
693 effectors, HopM1 and AvrE, create an aqueous apoplast in a humidity-dependent
694 manner. AvrE is localized to the host plasma membrane (PM)²³; its host target is
695 currently unknown. HopM1 targets MIN7 (an ARF-GEF protein) in the trans-Golgi-
696 network/early endosome (TGN/EE), which is involved in recycling of PM proteins²⁶.

697

698 **Extended Data Figure 5:** **a**, Col-0 leaves were syringe-infiltrated with *Pst* DC3000
699 (1×10^6 cfu/ml) or *Pst* DC3000 (*avrRpt2*) (1×10^7 cfu/ml). Plants were kept under high
700 humidity (~95%) for 24 h to observe water soaking and then shifted to low humidity
701 (~25%) for 2 h to observe ETI-associated tissue collapse. Pictures were taken before
702 and after low humidity exposure (**a**) and bacterial populations were determined 24 h
703 post infiltration to show similar population levels (**b**). * indicates a significant difference
704 of bacterial population, as determined by Student's *t*-test (two-tailed); *, $p=0.033$. $n=3$
705 technical replicates; error bars, mean \pm s.d. Experiments were repeated three times. This
706 is an experimental replicate of Fig. 3**b** and 3**c** (without *rps2*).

707

708 **Extended Data Figure 6:** Characterization of the *npr1-6* mutant. **a**, A diagram
709 showing the T-DNA insertion site in the *npr1-6* mutant. Blue boxes indicate exons in the
710 *NPR1* gene. **b**, RT-PCR results showing that the *npr1-6* line cannot produce the full-
711 length *NPR1* transcript. Primers used (*NPR1* sequence is underlined): *NPR1*-F:
712 agaattcATGGACACCACCATTGATGGA; *NPR1*-R: agtcgacCCGACGACGATGAGAGARTTTAC;
713 *UBC21*-F: TCAAATGGACCGCTCTTATC; *UBC21*-R: TCAAATGGACCGCTCTTATC.
714 Uncropped gel images are included in Supplementary Figure 1. **c**, The *npr1-6* line,
715 similar to *npr1-1*, is greatly compromised in benzothiadiazole (BTH)-mediated resistance
716 to *Pst* DC3000 infection. The Col-0, *npr1-1* and *npr1-6* plants were sprayed with 100µM
717 BTH and, 24 h later, dip-inoculated with *Pst* DC3000 at 1×10^8 cfu/ml. Bacterial
718 populations were determined 3 days post inoculation. * indicates a significant difference
719 between mock and BTH treatment, as determined by Student's *t*-test (two-tailed); *,
720 $p=0.027$; ***, $p=1.6 \times 10^{-4}$; ns, not significant ($p=0.19$). $n=3$ technical replicates; error
721 bars, mean \pm s.d. Experiments were repeated three times.

722 **Extended Data Figure 7:** Construction and characterization of the *mfec* and *mbbc*
723 quadruple mutants. **a**, CRISPR-Cas9-mediated mutations in the 4th exon of the *MIN7*
724 gene (exons indicated by blue boxes) in the quadruple mutant lines used in this study.
725 The underlined sequence in the wild type (WT) indicates the region targeted by sgRNA.
726 The number "399" indicates the nucleotide position in the *MIN7* coding sequence. "+1"
727 and "-1" indicate frame shifts in the mutant lines. **b**, Col-0 and various mutants used in
728 this study have similar growth, development and morphology. Four-week-old plants are
729 shown. **c**, The *mfec* and *mbbc* plants show a tendency of developing sporadic water
730 soaking under high humidity. Five-week-old regularly-grown (~60% relative humidity)
731 Col-0, *mfec* and *mbbc* plants were shifted to high humidity (~95%) for overnight and
732 pictures of mature leaves were taken after high humidity incubation. **d**, Even leaves of
733 *mfec* and *mbbc* plants that do not have sporadic water-soaking have a tendency to
734 develop some water soaking after *hrcC* inoculation. Five-week old Col-0, *mfec* and
735 *mbbc* plants were dip-inoculated with *hrcC* at 1×10^8 cfu/ml, and kept under high
736 humidity (~95%). Leaf pictures were taken 2 days post inoculation. Images were

737 representative of leaves from at least four plants. **e**, The non-pathogenic *hrcC* mutant
738 causes significant necrosis and chlorosis in the quadruple mutant plants. Col-0, *mfec*
739 and *mbbc* plants were dip-inoculated with the *hrcC* strain at 1×10^8 cfu/ml. Pictures
740 were taken 9 days post inoculation. This is one of the four independent experimental
741 repeats of the results presented in Fig. 5b.

742 **Extended Data Fig. 8: a**, Increased endophytic bacterial community in the *mfec* and
743 *mbbc* plants depend on high humidity. Col-0, *mfec* and *mbbc* plants were either
744 sprayed with H₂O and kept under high humidity (~95%) or kept under low humidity
745 (~50%). On day 5, total populations of the endophytic bacterial community were
746 quantified. Statistical analysis was performed by one-way ANOVA with Tukey's test (p
747 value set at 0.05). Bacterial populations indicated by different letters (i.e., a and b) are
748 significantly different. *n*=4 technical replicates; error bars, mean \pm s.d. Experiments were
749 repeated three times. **b**, Mild chlorosis and necrosis in leaves is associated with
750 increased endophytic bacterial community level in the *mfec* and *mbbc* quadruple mutant
751 plants. Plants were sprayed with H₂O and kept under high (~95%) humidity. Pictures
752 were taken 10 days after spray. Individual leaves are enlarged and shown in the lower
753 panel, showing mild chlorosis and necrosis in some of the *mfec* and *mbbc* leaves.

754 **Extended Data Fig. 9:** Validation of 1 min as an effective surface sterilization time.
755 Five-week old Col-0 plants were sprayed with H₂O and kept under high humidity
756 (~95%) for 5 days. Leaves were detached, surface sterilized in 75% ethanol for 20s,
757 40s, 1min or 2min and then rinsed in sterile water twice. No sterilization (0s) was used
758 as control. Leaves were ground in sterile water and bacterial numbers were determined
759 by serial dilutions and counting of colony-forming units on R2A plates. Statistical
760 analysis was performed by one-way ANOVA with Tukey's test (p value set at 0.05).
761 Bacterial populations indicated by different letters (i.e., a and b) are significantly
762 different. *n*=4 technical replicates; error bars, mean \pm s.d. Experiments were repeated
763 twice with similar results.

764

765 **Supplementary Information**

766 **Supplementary Video 1:** A movie showing the process of *Pst* DC3000 infection of
767 Arabidopsis plants. Five-week-old Col-0 plants were dip-inoculated with *Pst* DC3000 at
768 1×10^8 cfu/ml. Plants were kept under high humidity (~95%) and the disease symptoms
769 were recorded over 4 days. The process was sped up by 8,640-fold (24 h to 10
770 seconds). The recording started 7 h after inoculation and the red arrow indicates one
771 leaf, as an example, that showed the transient appearance of water soaking.

772

773 **Supplementary Figure 1:** Uncropped gel/blot images. Red boxes indicate cropped
774 sections that are used in the main or Extended Data figures. Diagram in **a** indicates how
775 the two gel blots in **b** and **c** were generated.

776

Fig. 1

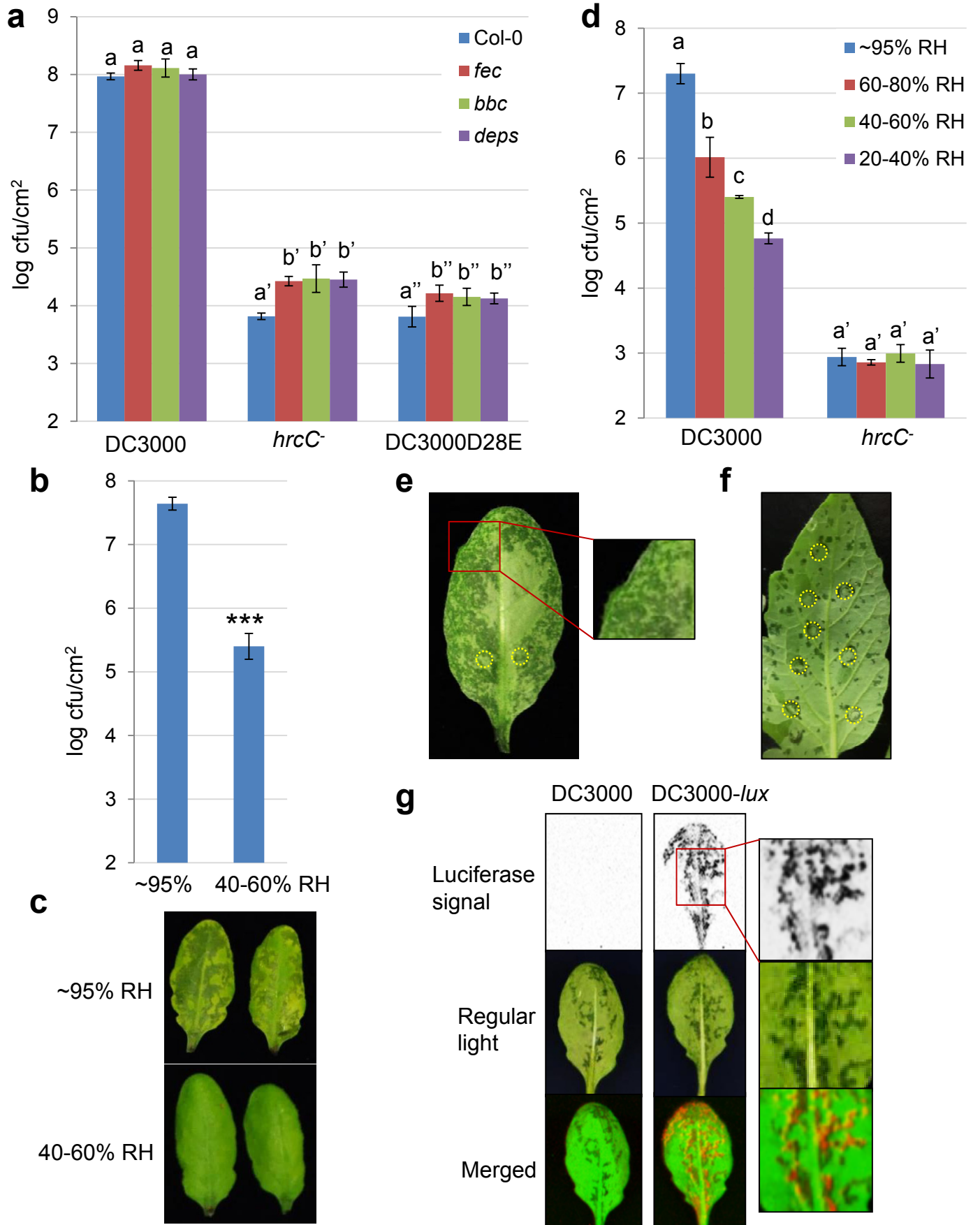


Fig. 2

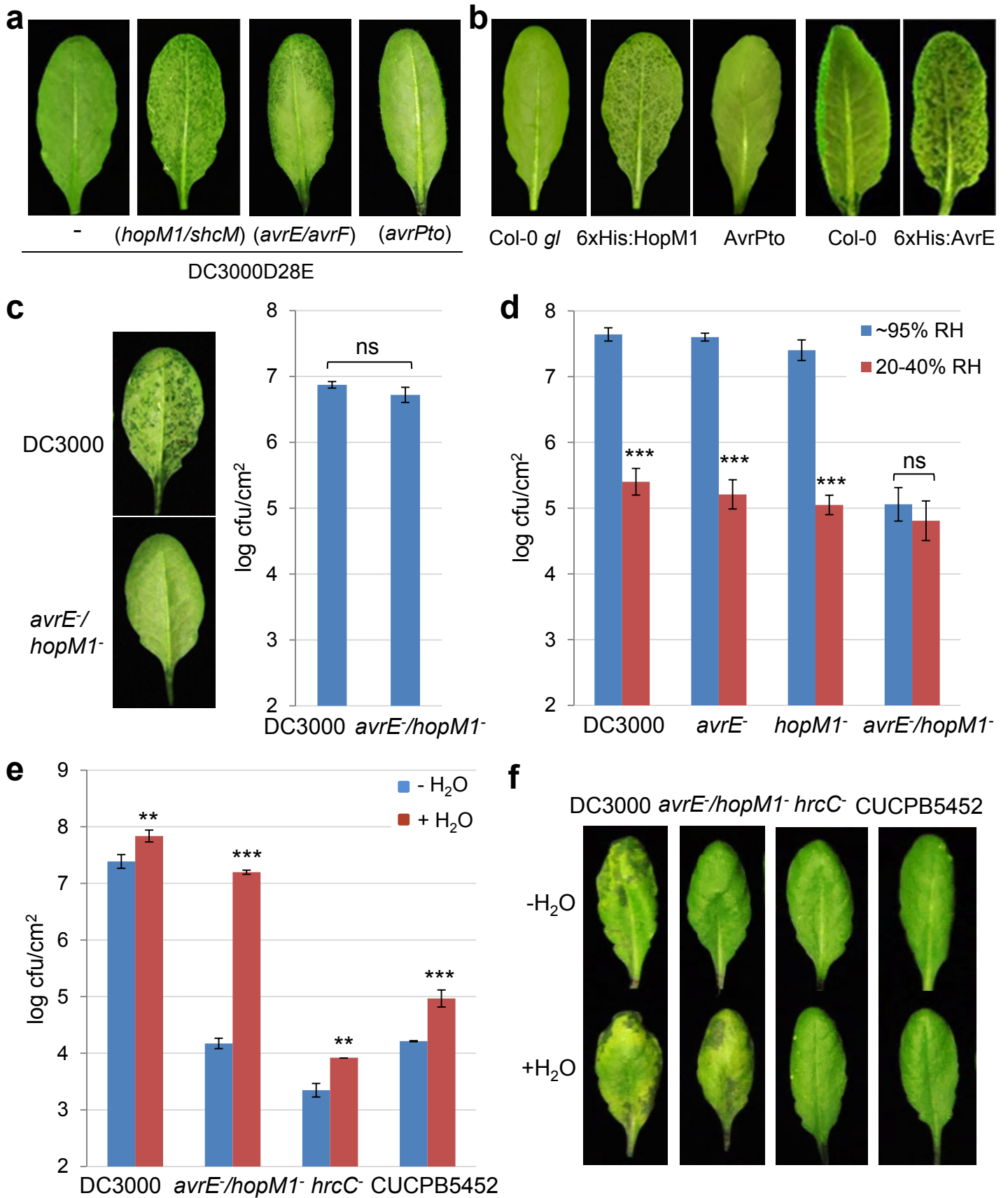


Fig. 3

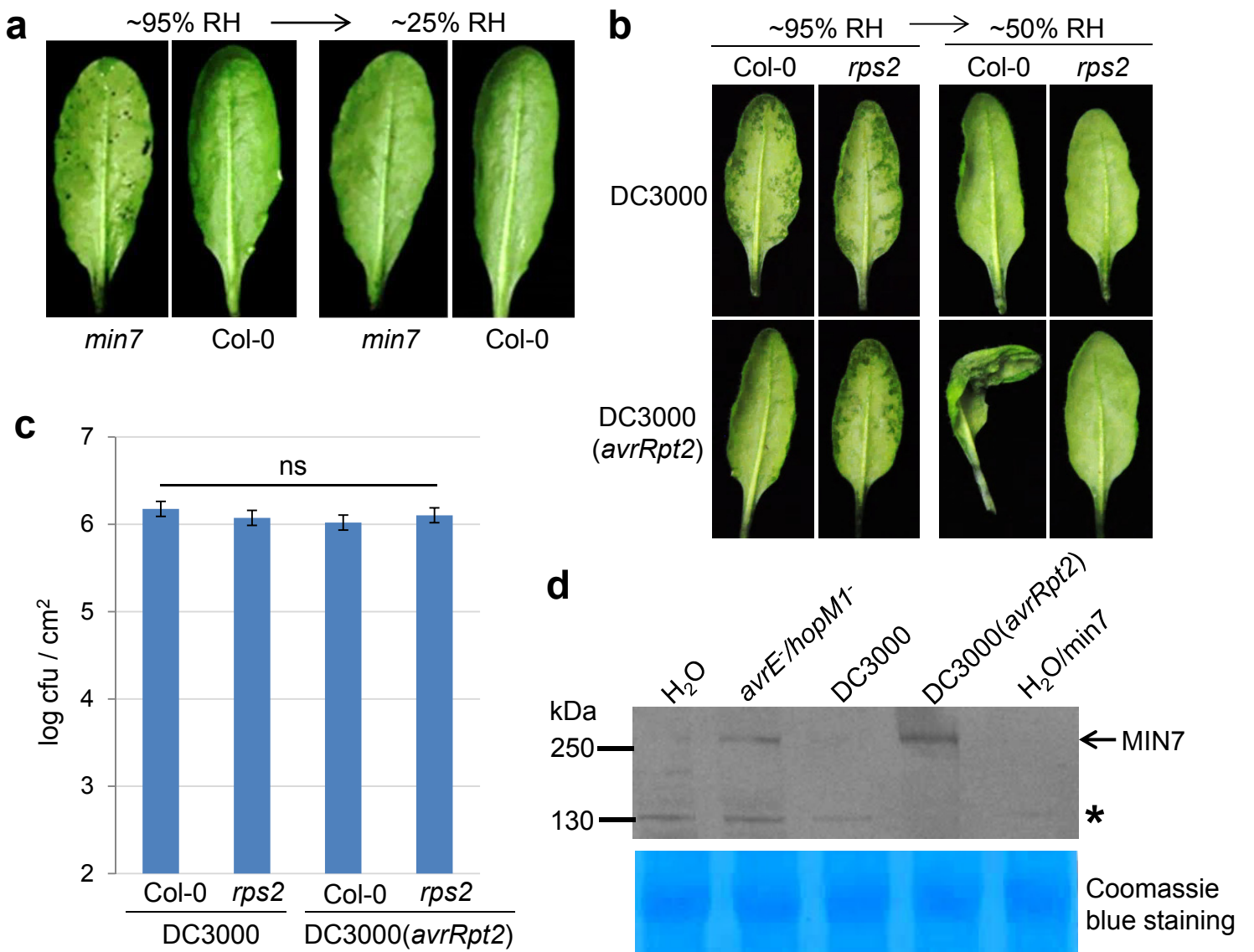


Fig. 4

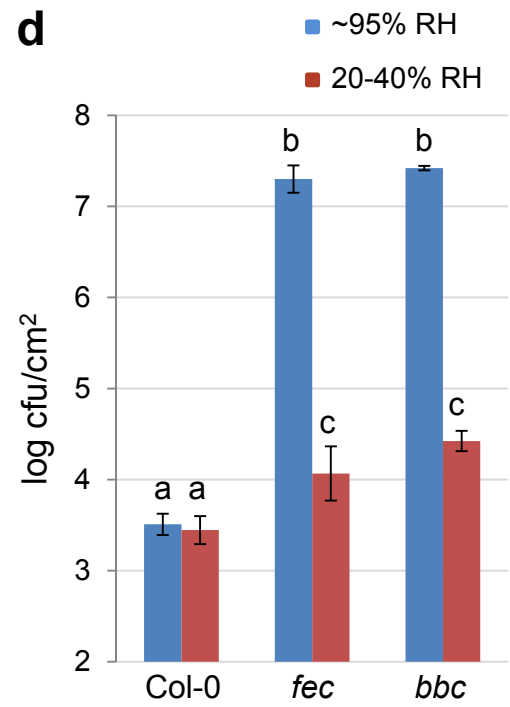
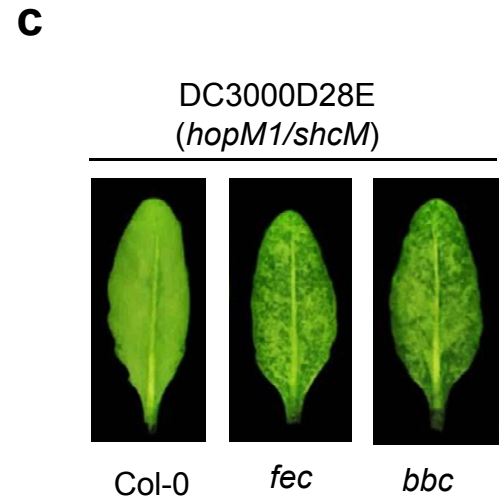
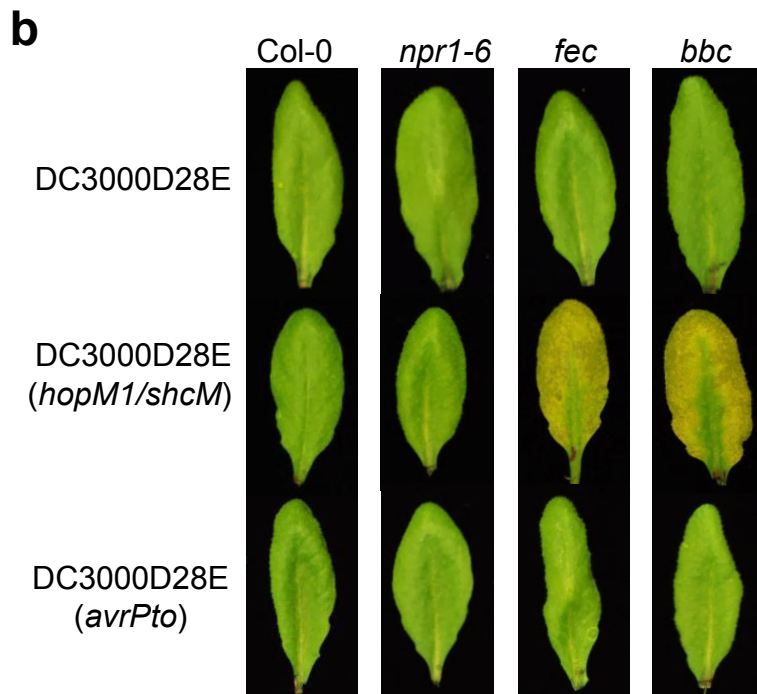
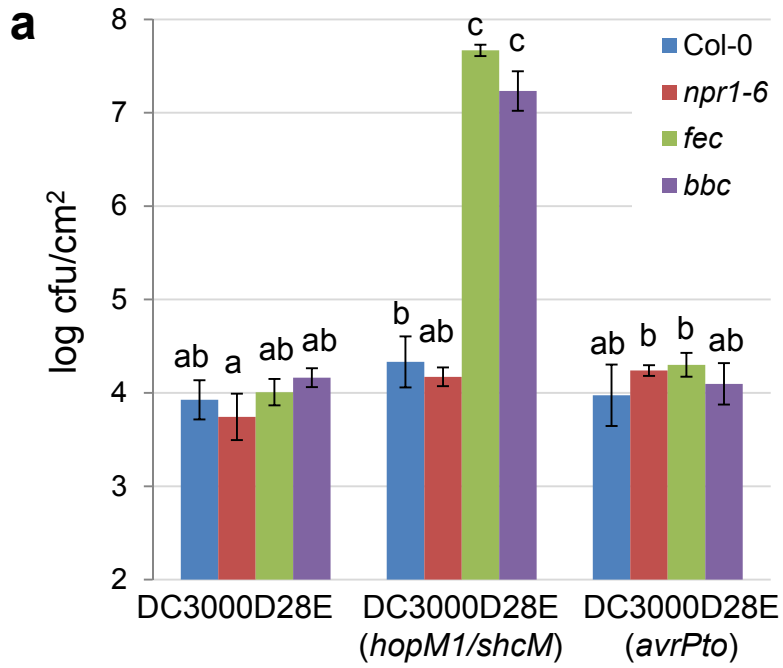
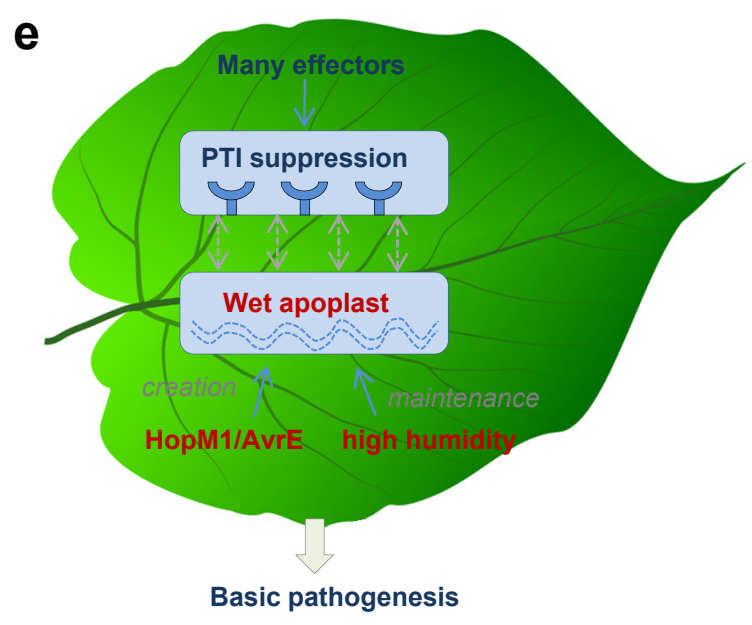
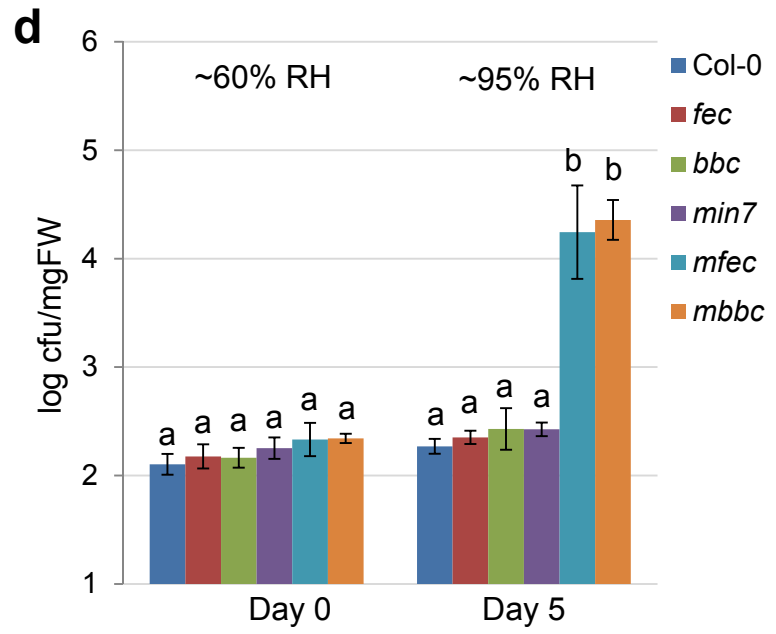
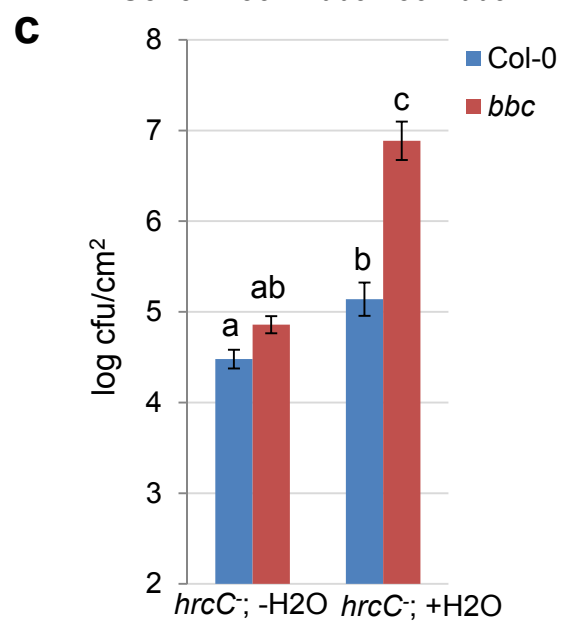
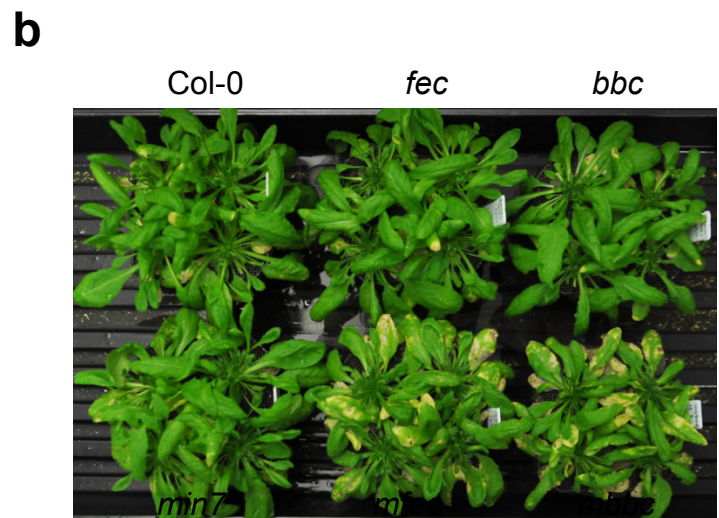
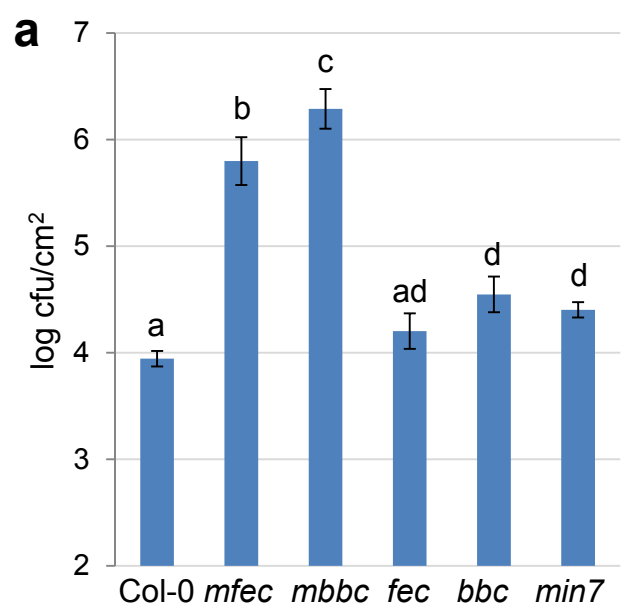


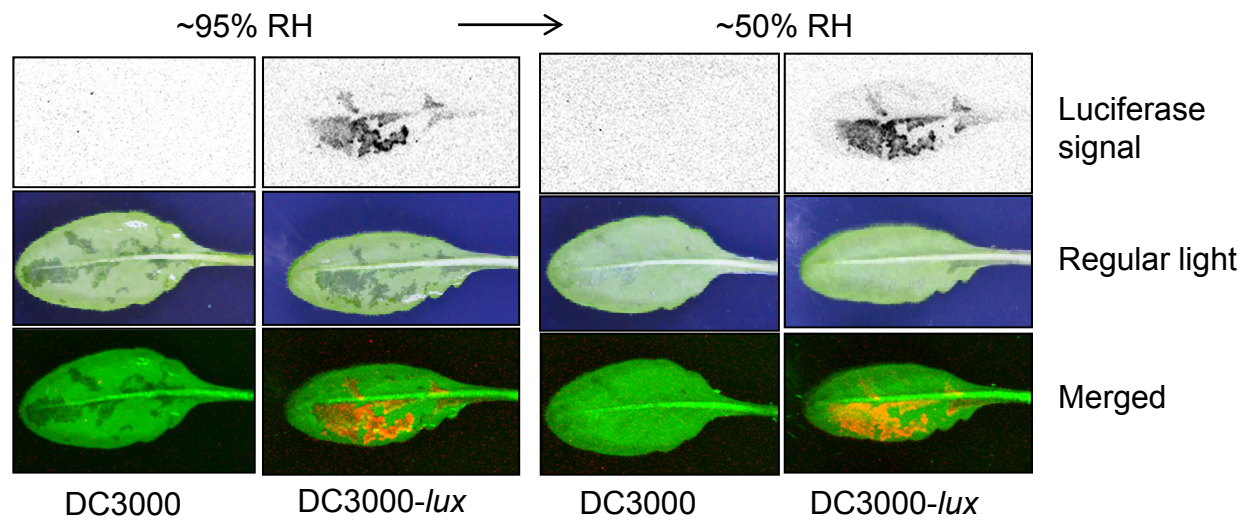
Fig. 5



Extended Data Table 1

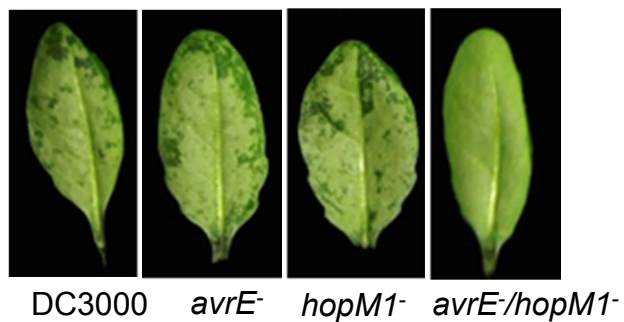
Order/Family	Col-0	<i>mfec</i>	<i>mbbc</i>
Bacillales			
Paenibacillaceae	15 (30%)	nd*	nd
Burkholderiales			
Comamonadaceae	8 (16%)	12 (24%)	9 (18%)
Burkholderiaceae	4 (8%)	1 (2%)	22 (44%)
Alcaligenaceae	3 (6%)	19 (38%)	12 (24%)
Flavobacteriales			
Flavobacteriaceae	6 (12%)	1 (2%)	1 (2%)
Xanthomonadales			
Xanthomonadaceae	4 (8%)	9 (18%)	nd
Sphingomonadales			
Sphingomonadaceae	3 (6%)	nd	1 (2%)
Sphingobacteriales			
Sphingobacteriaceae	3 (6%)	nd	nd
Chitinophagaceae	1 (2%)	nd	nd
Rhizobiales			
Rhizobiaceae	2 (4%)	5 (10%)	nd
Cytophagales			
Cytophagaceae	1 (2%)	nd	nd
Pseudomonadales			
Pseudomonadaceae	nd	1 (2%)	5 (10%)
Actinomycetales			
Microbacteriaceae	nd	2 (4%)	nd

Extended Data Fig. 1



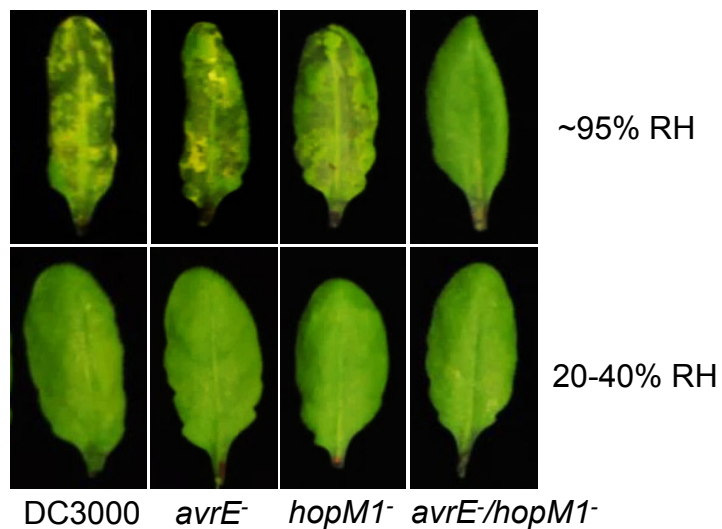
Extended Data Fig. 2

a



DC3000 *avrE*⁻ *hopM1*⁻ *avrE*⁻/*hopM1*⁻

b



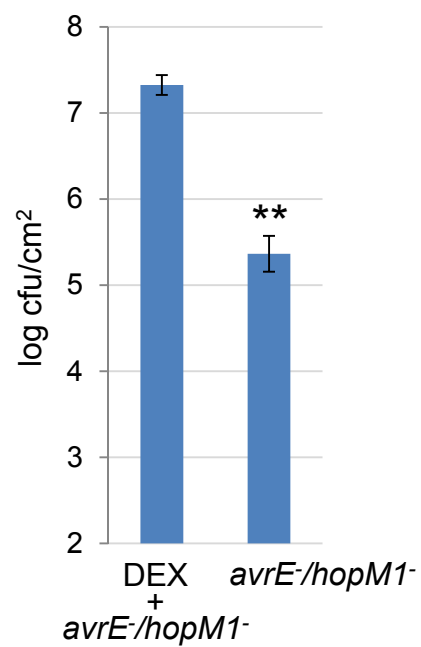
DC3000 *avrE*⁻ *hopM1*⁻ *avrE*⁻/*hopM1*⁻

c

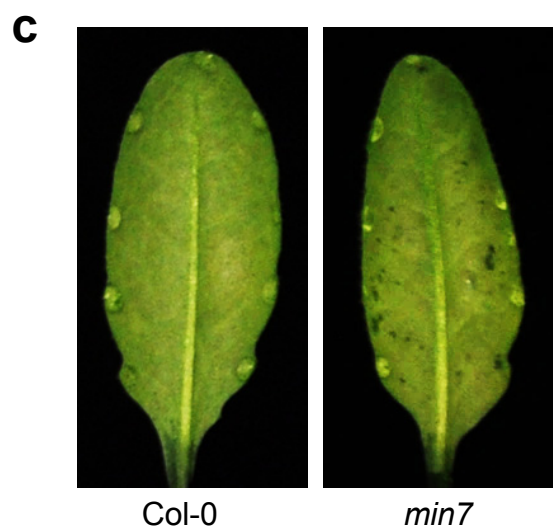
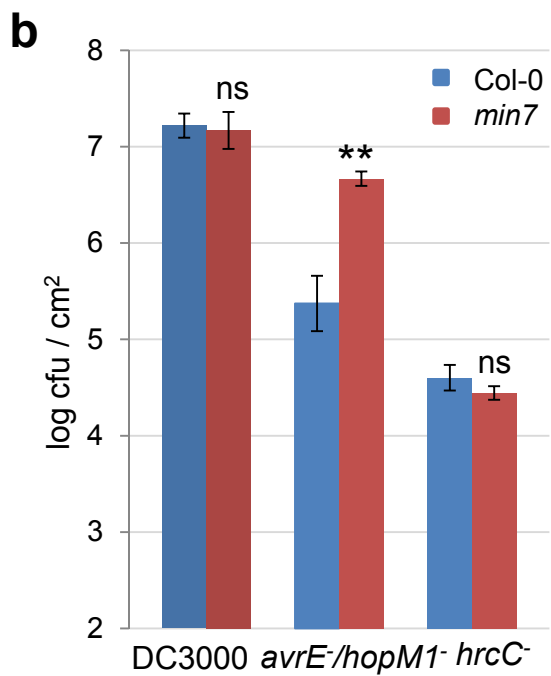
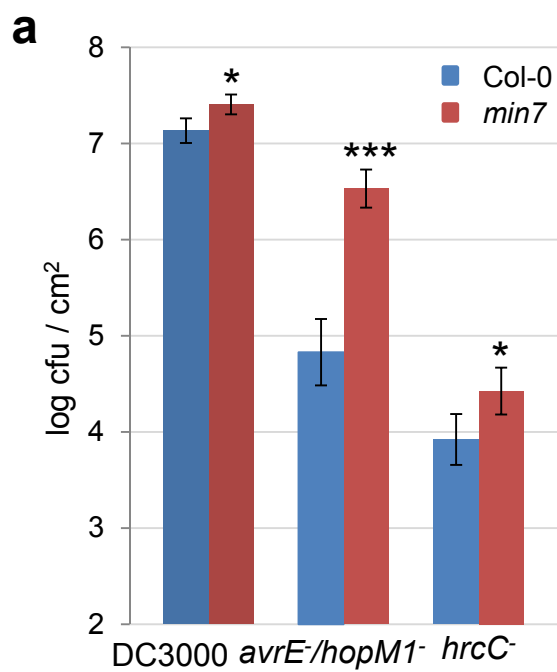


DEX DEX *avrE*⁻/*hopM1*⁻ H₂O
+
avrE⁻/*hopM1*⁻

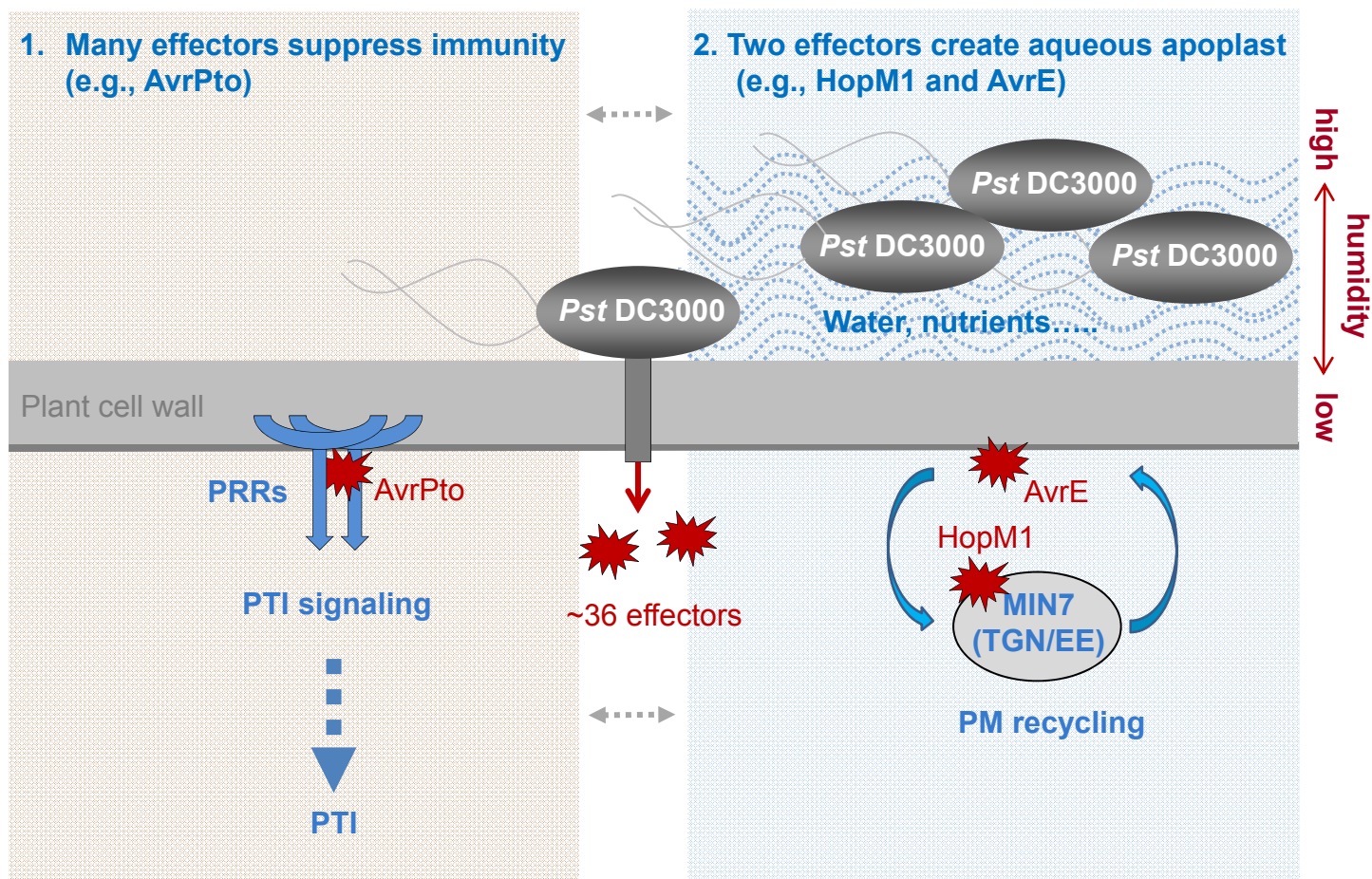
d



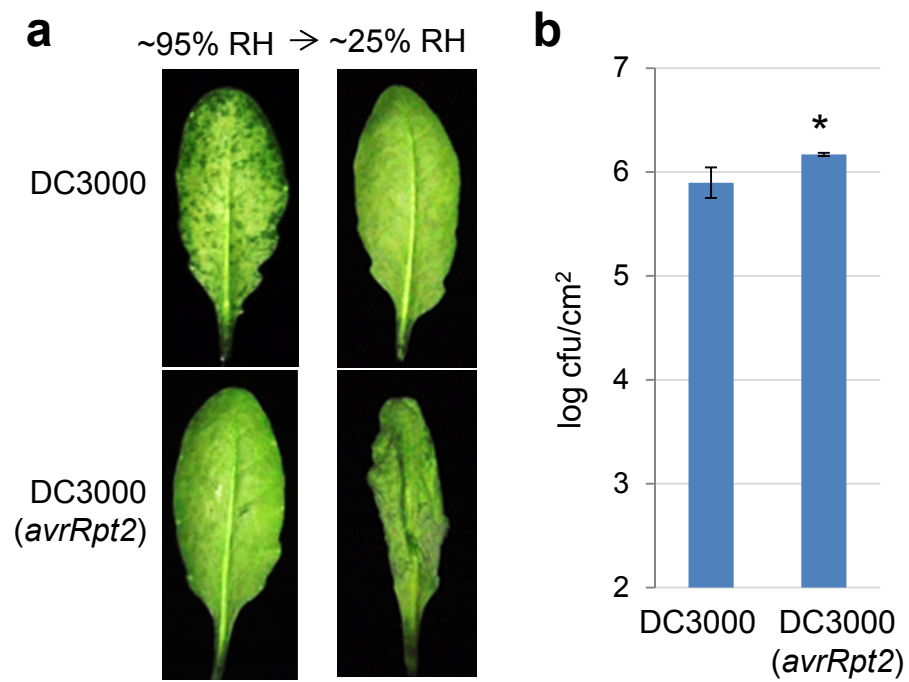
Extended Data Fig. 3



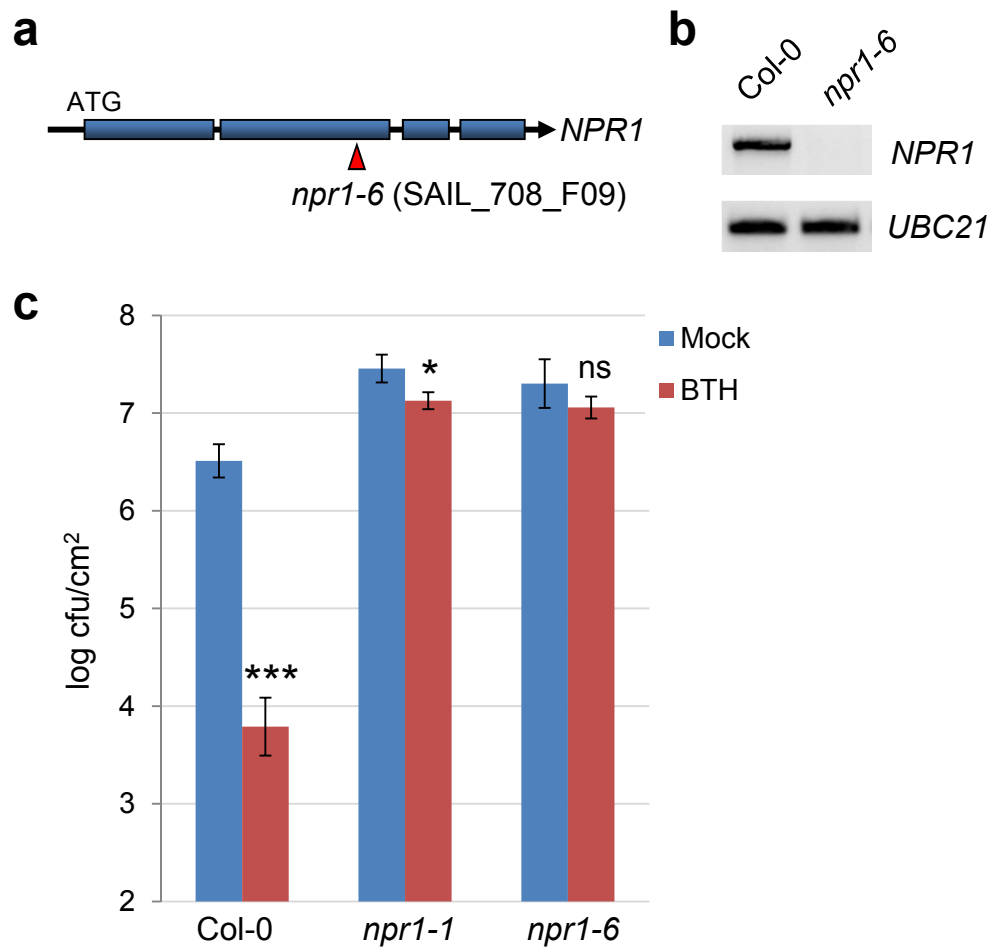
Extended Data Fig. 4



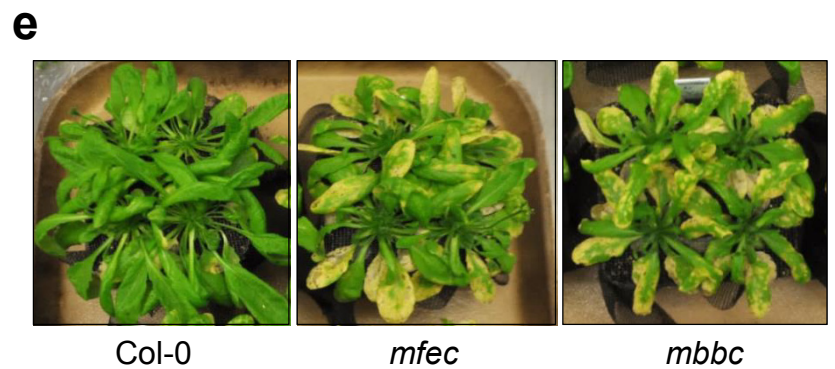
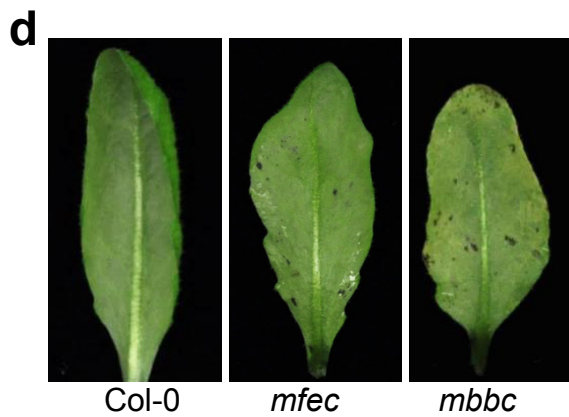
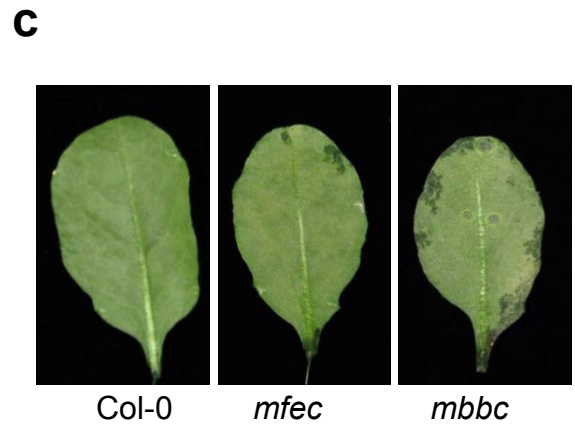
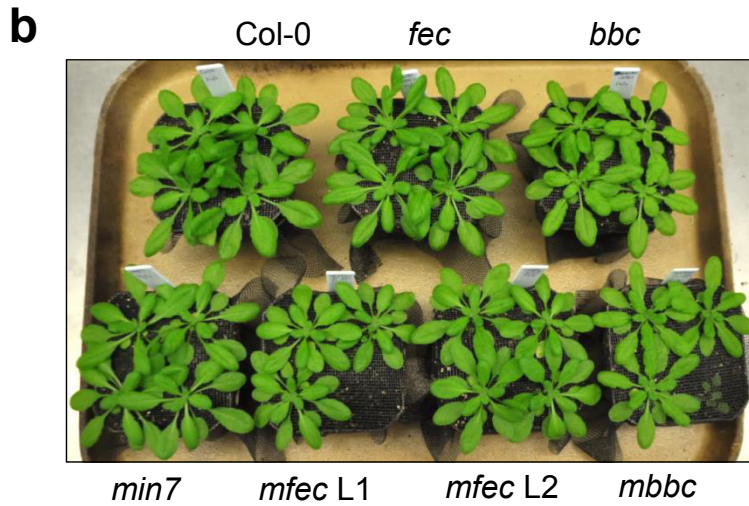
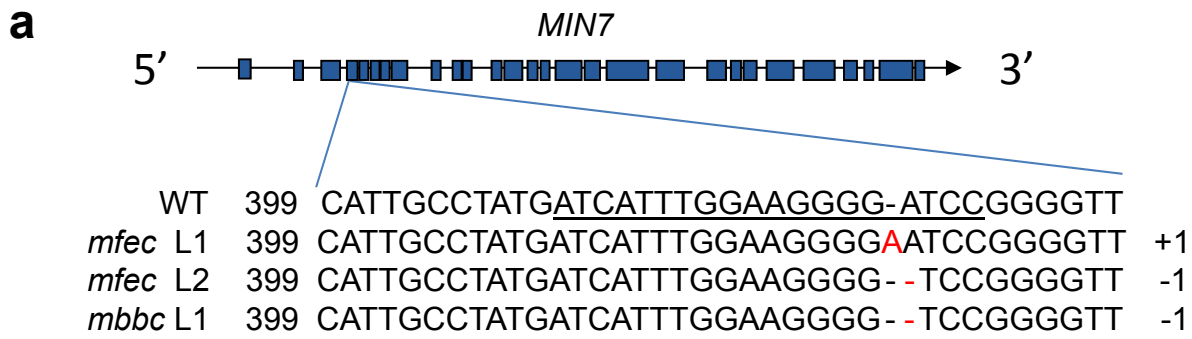
Extended Data Fig. 5



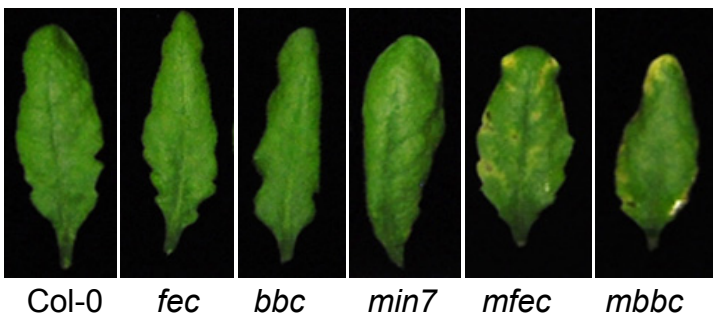
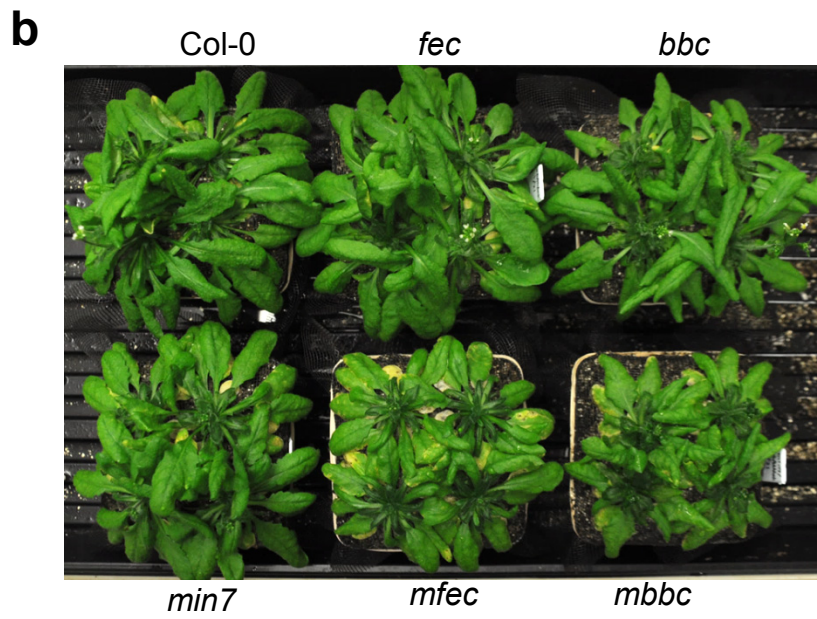
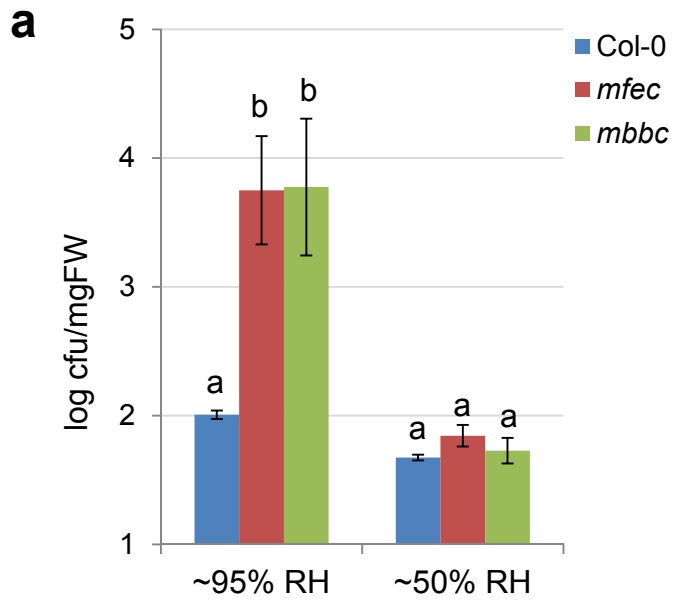
Extended Data Fig. 6



Extended Data Fig. 7



Extended Data Fig. 8



Extended Data Fig. 9

